

正および負の電荷のミューオンの物質中の寿命 Lifetime of Positive and Negative Muons in Matter

Suguru Tamamushi

August 14, 2014

Abstract

Positive and negative muons have different lifetimes in matter. This is due to the formation of muonic atoms in matter and subsequent nuclear capture in the case of negative muons. Positive muons decay into a positron, an electric neutrino, and an anti-mu-neutrino. Its lifetime is always $2.2 \mu\text{s}$. Negative muons in muonic atoms either decay or are captured by nuclei. When it decays, it decays into an electron, anti-electric-neutrino and a mu-neutrino. When it is captured by the nuclei, either a neutron is emitted or the nucleus is excited, in addition to an anti-neutrino emission. The excited nucleus then emits protons, neutrons, or other particles. The lifetime of negative muons in matter depends on the atomic number Z of the material and it is shorter than the lifetime of positive muons.

In the present research, I tested whether the decays of both positive and negative muons can be observed using cosmic ray muons. I measured the lifetime of cosmic ray muons stopped in aluminum and iron. I measured the time spectra by recording the time difference between the incoming muon and the outgoing decay electron or positron with plastic scintillators. With my setup, I was able to substantially reduce the number of background events compared to earlier setups as I used coincidence both for the start and stop signals of the time spectra.

Hints for a shorter negative muon lifetime were observed by these measurements. The negative muon lifetime measured in the present experiment is in agreement with the expected value in aluminum.

Contents

1	Introduction	3
2	Decay of Positive and Negative Muons	4
2.1	Decay of Positive Muons	4
2.1.1	Decay	4
2.1.2	Lifetime of Positive Muons	5
2.2	Decay of Negative Muons	6
2.2.1	Muonic Atoms	6
2.2.2	Lifetime of Negative Muons	7
2.3	Cosmic Ray Muons	8
3	Experimental Setup	12
3.1	Setup	12
3.2	Plastic Scintillator	12
3.3	Photomultiplier Tube	15
3.4	Materials used as stopper	16
3.4.1	Interaction of muons with matter	17
3.4.2	Interaction of electrons with matter	18
3.4.3	Optimization of material thickness	18
3.5	Electronics and Circuitry	19
3.5.1	Modules	19
3.5.2	Circuit	20
4	Preparations for Measurements	23
4.1	Time Calibration	23
4.2	Discriminator Threshold	24
4.3	Coincidence, Anti-coincidence and Accidental Coincidence	26
4.3.1	Coincidence and Anti-coincidence	27
4.3.2	Accidental Coincidence	27
5	Muon Lifetime Measurements	28
5.1	Positive Muon Lifetime Measurement	28
5.1.1	Measurement	28
5.1.2	Fit	28
5.2	Negative Muon Lifetime Measurement	30
5.2.1	Measurement	30
5.2.2	Fit	30
6	Analysis of Data	32
6.1	Reduction of Background	32
6.2	Results of Positive Muon Lifetime Measurement	35
6.3	Results of Negative Muon Lifetime Measurement	38
6.3.1	Using $2.2 \mu\text{s}$ as the positive muon lifetime	38

6.3.2	Using $2.1 \mu\text{s}$ as the positive muon lifetime	41
6.3.3	Using $2.0 \mu\text{s}$ as the positive muon lifetime	44
6.3.4	Using $2.3 \mu\text{s}$ as the positive muon lifetime	46
7	Conclusion and Summary	49

1 Introduction

In the present research, the lifetime of muons in aluminum and iron was measured. The lifetime of negative muons in material is different from the lifetime of negative muons in vacuum. The difference is due to the formation of muonic atoms in matter and subsequent nuclear capture.

The purpose of my research is as follows:

1. To understand the basics of plastic scintillators, coincidence, anti-coincidence and accidental coincidence using cosmic ray muons.
2. To test whether decays of positive and negative muons in materials can be observed using cosmic ray muons. Cosmic ray muons are a mixture of positive and negative muons. Cosmic ray muons were stopped in aluminum and iron. Aluminum was used to test whether the lifetime of negative muons can be observed. Iron was used to test whether the lifetime of positive muons can be measured.

The structure of this thesis is as follows. In chapter 1, the purpose of the present research and the structure of the thesis are explained. In chapter 2, the basic information regarding the decays of positive and negative muons, and cosmic ray muons are described. In chapter 3, the experimental setup and the apparatus used is explained. In chapter 4, preparations for the measurement are explained. Specifically, the time calibration for the TAC + ADC, the discriminator threshold setting, and coincidence are explained. In chapter 5, the procedure for measuring the lifetimes of positive and negative muons are described. In chapter 6, the data is analyzed. In chapter 7, the conclusion is described and the thesis is summarized.

2 Decay of Positive and Negative Muons

Muons are elementary particles and constitute one of the three generations of charged leptons. Muons have 1/2 spin. There are two types of muons: positive muons, μ^+ , with electric charge +1 and negative muons, μ^- , with electric charge -1. Since the discovery of muons in 1936 in cosmic rays, the characteristics of muons have been extensively studied. It was first considered to be a candidate of Yukawa particle which mediates the nuclear force, but later turned out to be a lepton. The mass of muons m_μ compiled by the Particle Data Group is

$$m_\mu = 105.6583715 \pm 0.0000035 \text{ MeV.} \quad (1)$$

The mass of muons is about 200 times larger than the mass of electrons and positrons.

The lifetime of muons is explained by the V-A (vector-axial vector) theory of weak interaction. The decay width Γ for a free decay is expressed as

$$\Gamma = \frac{\hbar}{\tau} = \frac{G_F^2}{192\pi(\hbar c)^6} \cdot (m_\mu c^2)^2 \cdot (1 + \epsilon) \quad (2)$$

where τ is the lifetime, G_F Fermi coupling constant, m_μ the mass of muons, and ϵ a correction for the higher order processes. In the present research, the lifetime of muons in material is studied. The lifetime of positive and negative muons in several materials are listed in Table 1 [4].

Material	Atomic Number Z	Lifetime of μ^+ (μ s)	Lifetime of μ^- (μ s)
Free Decay	0	2.2	2.2
Carbon	6	2.2	2.0
Aluminum	13	2.2	0.88
Iron	26	2.2	0.20
Lead	82	2.2	0.08

Table 1: The lifetimes of positive and negative muons in different materials. The lifetime of positive muons is always $2.2 \mu\text{s}$, while the lifetime of negative muons depends on the atomic number Z of the materials.

2.1 Decay of Positive Muons

2.1.1 Decay

Positive muons decay as

$$\mu^+ \rightarrow e^+ + \nu_e + \bar{\nu}_\mu. \quad (3)$$

The Feynman diagram of the decay is shown in Fig. 1.

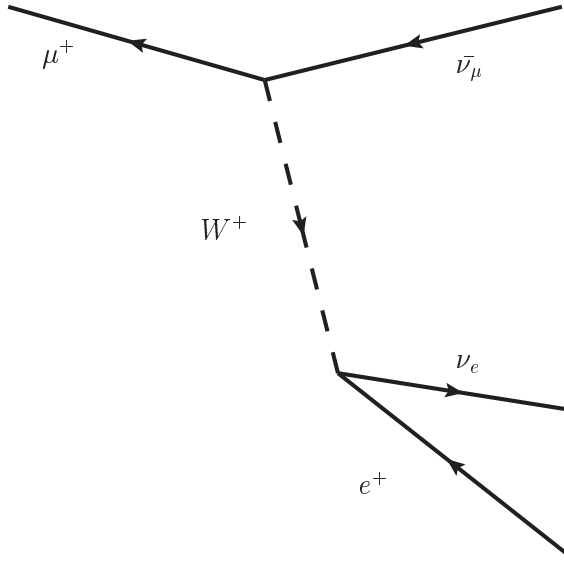


Figure 1: The Feynman diagram of the decay of a positive muon. Positive muons decay into an anti-mu-neutrino, a positron and an electric neutrino. The decay is mediated by a W^+ boson.

The number of remaining positive muons over time $N^+(t)$ is expressed as

$$N^+(t) = N_0^+ \exp(-t/\tau^+) \quad (4)$$

where N_0^+ is the initial number of positive muons.

Therefore the number of muons which have decayed, N_{decay}^+ , can be expressed as

$$N_{decay}^+ = N_0^+ - N^+(t) \quad (5)$$

$$= N_0^+ - N_0^+ \exp(-t/\tau^+). \quad (6)$$

The time derivative of N_{decay} is then

$$\frac{dN_{decay}^+}{dt} = \frac{N_0^+}{\tau^+} \exp(-t/\tau^+) \quad (7)$$

This shows the number of decay events in unit time. In the present research, this equation is used to determine the muon lifetime.

2.1.2 Lifetime of Positive Muons

The lifetime of the positive muon τ^+ compiled by Particle Data Group is

$$\tau^+ = 2.1969811 \pm 0.0000022 \text{ } \mu\text{s}. \quad (8)$$

For the present experiment, $2.2 \text{ } \mu\text{s}$ is used as the lifetime of positive muons. The lifetime of positive muons is always the same and does not depend whether the muon is in matter or in vacuum. The decay time spectrum of the muons stopped in iron is fitted with Eq. 7 to determine the lifetime of positive muons.

2.2 Decay of Negative Muons

The lifetime of negative muons in matter is different from the lifetime of negative muons in vacuum because the negative muons interact with the nuclei of atoms. In vacuum, the negative muon decays as follows:

$$\mu^- \rightarrow e^- + \bar{\nu}_e + \nu_\mu. \quad (9)$$

The ratio of positive muon lifetime to negative muon lifetime in vacuum compiled by Particle Data Group is

$$\frac{\tau^+}{\tau^-} = 1.000024 \pm 0.000078. \quad (10)$$

In vacuum, the positive muon lifetime and negative muon lifetime agree within error. Therefore, they satisfy the CPT invariance principle.

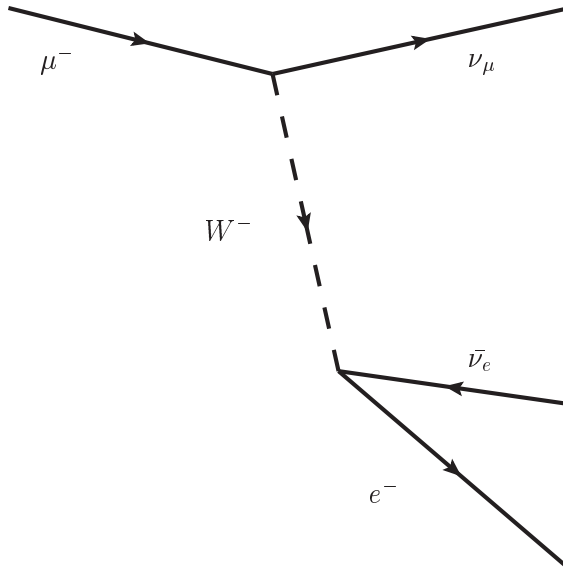


Figure 2: The Feynman diagram of the decay of a negative muon in vacuum. Negative muons decay into an electron, a mu-neutrino, and an anti-electric neutrino. The decay is mediated by a W^- boson.

2.2.1 Muonic Atoms

Negative muons are slowed down in matter and form muonic atoms. The muonic atom is an atom where an electron is replaced by a negative muon.

After the muonic atom is formed, the negative muon follows one of the following two processes:

1. Decay:

The negative muon decays in the same way as in vacuum.

$$\mu^- \rightarrow e^- + \bar{\nu}_e + \nu_\mu. \quad (11)$$

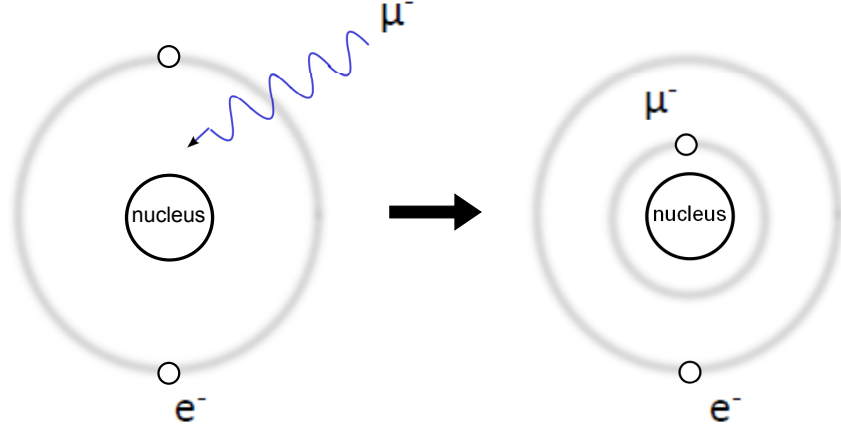


Figure 3: The schematic of a muonic atom. A negative muon comes in and replaces an electron orbiting around the nucleus. The negative muon then sits in its own orbit. The diameter of the orbit is smaller because the muon is heavier than an electron.

2. Nuclear Capture:

The negative muon is captured by the nucleus. The reaction is as follows:



or



In the process of Eq.12, the negative muon reacts with a proton 'p' in the nucleus and a neutron and a mu-neutrino are emitted. In the process of Eqs. (13 - 14), the negative muon reacts with a nucleus to create an excited nucleus and a mu-neutrino. The excited nucleus then emits protons, neutrons or other particles.

2.2.2 Lifetime of Negative Muons

The lifetime of negative muons is determined by those two competing processes. The lifetime of negative muons in free decay is denoted as τ_{decay}^- , and the lifetime of negative muons in nuclear capture is denoted as $\tau_{capture}^-$. The total lifetime of negative muons in a muonic atom is τ_{total}^- . The relation between the three is

$$\frac{1}{\tau_{total}^-} = \frac{1}{\tau_{decay}^-} + \frac{1}{\tau_{capture}^-} \quad (15)$$

The total decay rate of negative muons, Γ_{total} , in a muonic atom is expressed as

$$\Gamma_{total} = \frac{1}{\tau_{total}^-} = \Gamma_{decay} + \Gamma_{capture}. \quad (16)$$

where

$$\Gamma_{decay} = \frac{1}{\tau_{decay}^-} \quad (17)$$

is the decay rate of negative muons in a free decay and

$$\Gamma_{capture} = \frac{1}{\tau_{capture}^-} \quad (18)$$

is the rate of disappearance of negative muons by nuclear capture. The lifetime of negative muons depends on the atomic number Z of the matter. This is because the nuclear capture rate $\Gamma_{capture}$ depends on the atomic number Z . The nuclear capture rate and the atomic number Z are known to follow a simple relation in matter ($Z < 100$) [3]:

$$\Gamma_{capture} = \Gamma_1 \cdot Z^4 \quad (19)$$

where Γ_1 is the nuclear capture rate of negative muons in hydrogen. The rate of the nuclear capture is determined by the overlap between the wave function of the muon in the muonic atom and the nucleus. It means that the density of the muon at origin $|\psi(0)|^2$ determines the capture rate. This is the reason for the Z^4 dependence.

It is important to note that always the τ_{total} is measured in experiments. I will explain it in what follows. If electrons from decay are detected, τ_{total} is measured. If neutrons or protons from nuclear capture are detected, τ_{total} is measured.

The lifetime of negative muons in materials is different from material to material. A list of lifetimes in some materials are shown in Table 2.

Material	Z	Decay Lifetime (μs)	Capture Lifetime (μs)	Total Lifetime (μs)
Free Decay	0	2.2	-	2.2
Hydrogen	1	2.2	2.4×10^3	2.2
Carbon	6	2.2	25	2.0
Aluminum	13	2.2	1.5	0.88
Iron	26	2.2	0.22	0.20
Lead	82	2.2	0.09	0.08

Table 2: The lifetime of decay and nuclear capture and the total lifetime of negative muons in different materials. The lifetime of negative muons decreases as the atomic number Z of the material increases.

2.3 Cosmic Ray Muons

Particles from space entering Earth's atmosphere are called cosmic rays. A main source for the cosmic rays is the sun, but the origins of cosmic rays from outside the solar system

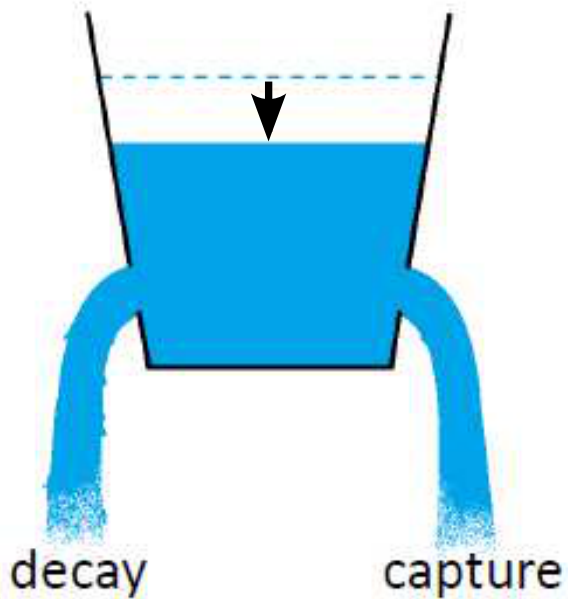


Figure 4: The negative muon decay rate is similar to the speed of water flowing from two holes in a bucket of water. The decay rate and capture rate cannot be separately measured. Only the total decay rate is measured. The rate of the decrease of the total water level is measured which ever channel one observes.

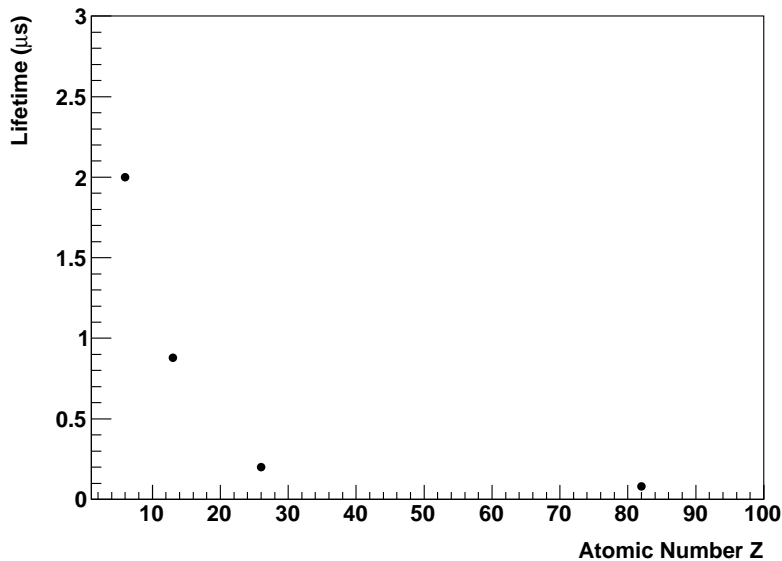


Figure 5: The negative muon lifetimes (τ_{total}^-) in different materials plotted against atomic number Z . The lifetime of negative muons in materials decreases as the atomic number Z increases. The lifetime of negative muons in carbon, aluminum, iron and lead are shown [4].

are not yet fully known. The energy of cosmic rays can be very high and some cosmic rays have been observed to have an energy of more than 10^{20} eV.

Most of the particles coming into the atmosphere are protons. Other particles are electrons and light nuclei such as helium or carbon. Those particles directly entering the atmosphere are called **primary cosmic rays**. They then hit the nitrogen or oxygen nuclei in the atmosphere and create hadrons or other particles. These particles created are called **secondary cosmic rays**. The secondary cosmic rays then continuously interact with the atoms in the atmosphere to create a shower of particles. The muons used in the present research comes from the showers. The muons mostly come from the decay of pions or kaons. The decays are as follows:

$$\pi^+ \rightarrow \mu^+ + \nu_\mu \quad (20)$$

$$\pi^- \rightarrow \mu^- + \bar{\nu}_\mu \quad (21)$$

$$K^+ \rightarrow \mu^+ + \nu_\mu \quad (22)$$

$$K^- \rightarrow \mu^- + \bar{\nu}_\mu \quad (23)$$

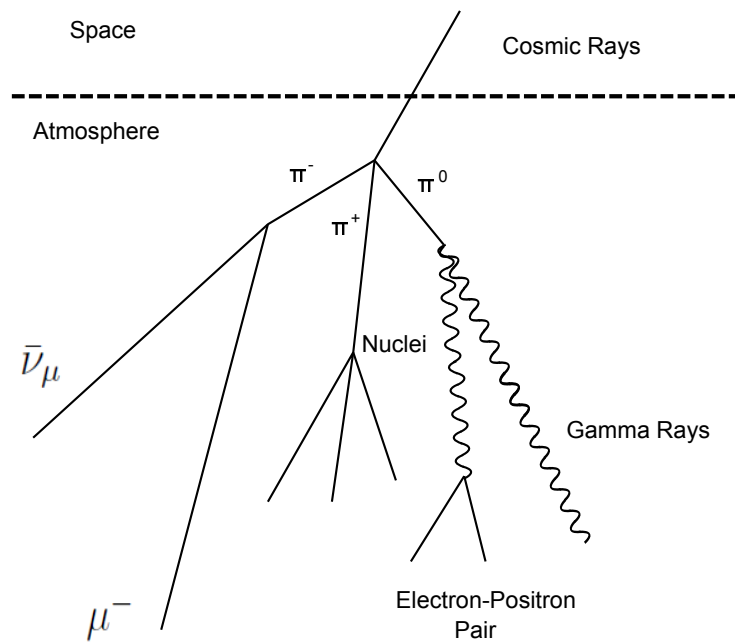


Figure 6: Primary cosmic rays enter the atmosphere and create a cascade of particles. Primary cosmic rays are mostly protons. They hit the nitrogen or oxygen nuclei in the atmosphere to create hadrons. Those hadrons then hit nuclei in the atmosphere again and create further particles.

The cosmic rays at the sea level contain a mixture of both positive and negative muons. The ratio of positive to negative muons is shown in Fig. 7 [5].

Muons reach the sea level at a rate of 1 muon/(min \times cm 2). In the present research, the experimental setup has an area of 144 cm 2 . Therefore, muons enter the setup at a rate of about 2.4 Hz.

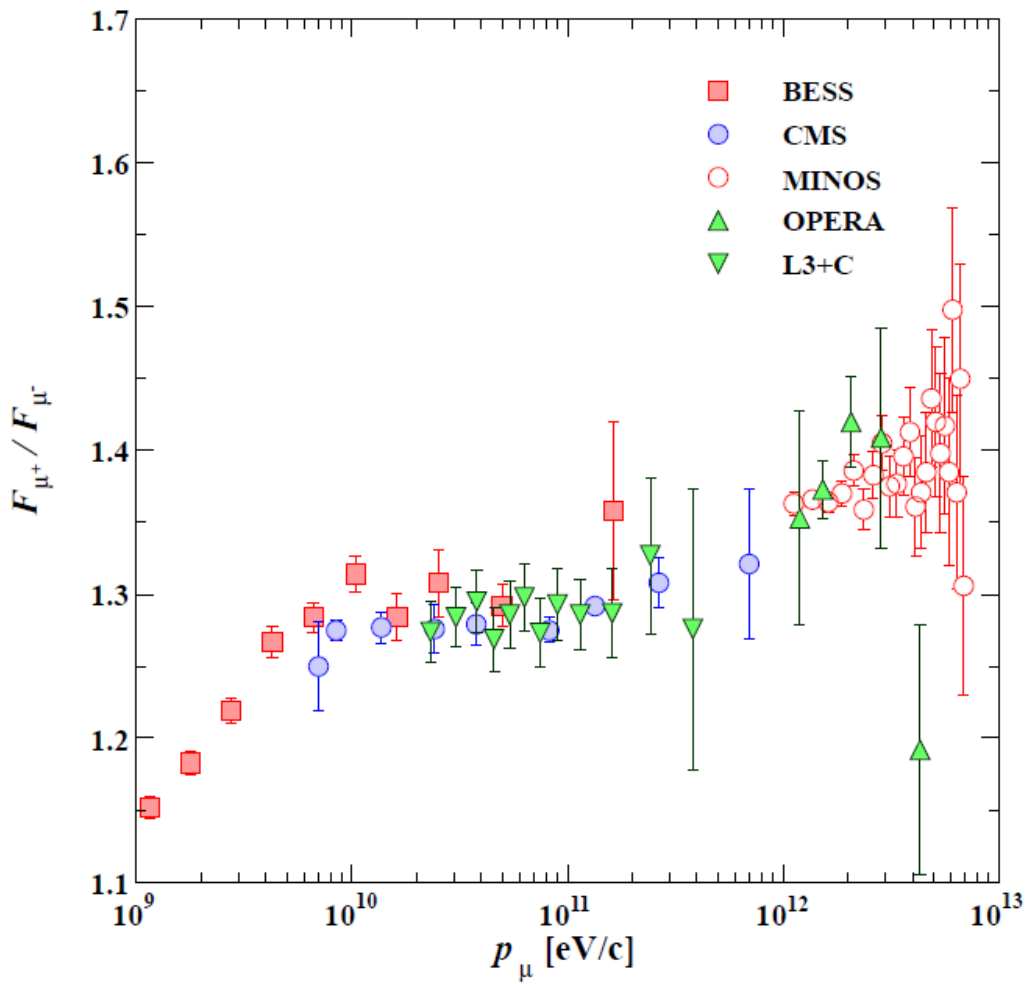


Figure 7: Ratio of positive to negative muons at different energy levels compiled by J. Beringer *et al.* (2013) [5]. The ratio μ^+/μ^- is greater than 1. The ratio is higher at higher energy.

3 Experimental Setup

3.1 Setup

The setup in this experiment is modified from earlier muon lifetime measurement experiments. The main improvements are:

1. Coincidence is used for the stop signal as well as for the start signal.
This coincidence is used to reduce backgrounds.
2. The setup is rearranged so that the materials can easily be exchanged.
The materials used to stop the muons could easily be changed. In this research, aluminum and iron are used.

As shown in Fig. 8, four plastic scintillators are connected to photomultiplier tubes. An incoming cosmic ray muon is detected using the top two plastic scintillators. A bottom plastic scintillator is used for anticoincidence. A part of muons stop in the material (in Fig. 8, aluminum is shown). The muon decays and emits an electron or a positron. The emitted electron or positron is detected by the top two or bottom two scintillators. The electron is recorded only if both #1 and #2 or both #3 and #4 generate signals. This requirement of coincidence reduces backgrounds.

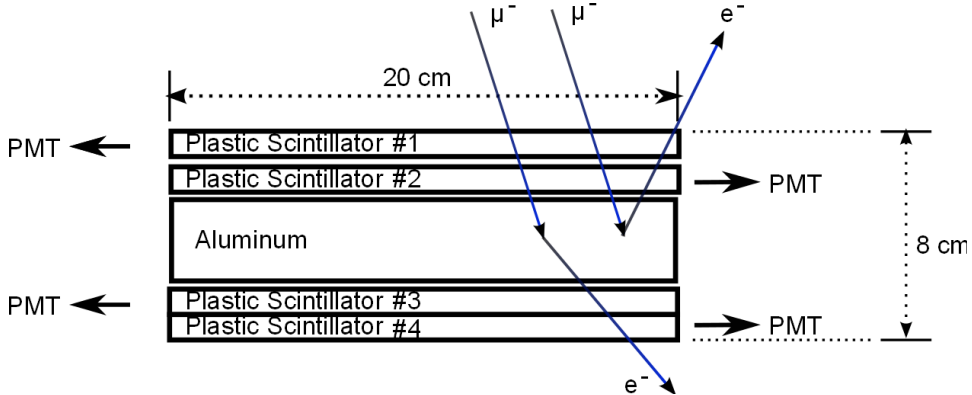


Figure 8: The schematics of the setup with aluminum as a stopper. The aluminum can be exchanged with iron easily. The muons penetrate the top two plastic scintillators and stop at the aluminum. The decay electron or positron is detected with the top two or bottom two scintillators.

The actual setup is shown in Fig. 9.

3.2 Plastic Scintillator

Scintillators are used in general to detect radiation and charged particles. There are mainly two types of scintillators: organic scintillators and inorganic scintillators. In the present experiment, plastic scintillators are used for the measurement of charged particles.



Figure 9: The actual setup used in the experiment. The photomultiplier tubes and the plastic scintillators are set on height-adjustable stands. The materials are placed on a wooden board.

The plastic scintillator is a typical example of organic scintillators.

1. Organic Scintillators

Organic scintillators are scintillators made from organic compounds. Organic scintillators have a quick response to particles. Therefore, organic scintillators are suited for measuring time spectra. There are two types of fluorescent materials widely used for organic scintillators: 1) anthracene and 2) stilbene. Most organic scintillators have the fluorescent materials mixed in other organic compounds depending on the use. Two examples of typical organic scintillators are plastic scintillators and liquid organic scintillators. Plastic scintillators use plastic to encase the fluorescent materials. Because plastic can be molded into a variety of shapes, many different shapes of plastic scintillators can be created. Plastic is also inexpensive and therefore allows large scintillators to be fabricated. Liquid organic scintillators use a liquid organic solvent to mix the fluorescent materials into. The advantage of liquid organic scintillators is that because it is liquid and does not have a definite shape, it is durable and can withstand particles with high energy. The scintillation process for organic compounds depends only on the compound used and does not depend on the physical state of the compound itself. Therefore, the same scintillator compound in a liquid state or a solid state will have the same scintillation process.

2. Inorganic Scintillators

Inorganic Scintillators are made from inorganic materials such as NaI or CsI. The scintillation process depends on the crystal structure of the inorganic compound. The advantage of inorganic scintillators is the linearity between the energy of the particle and the amount of scintillation light created. Therefore, inorganic scintillators are suited for measuring the energy of particles.

In this experiment, plastic scintillators are used to detect charged particles because measuring the timing of the particles is the main purpose. The plastic scintillators have been made by CI Kogyo, Inc. The plastic scintillators in the present experiment is made mostly of polyvinyltoluene and about 2 to 3% of a fluorescent substance. All the plastic scintillators are wrapped in aluminum miler and black vinyl to shield lights from outside. The dimensions are shown below.

Dimension (Length × Width × Depth)
20 cm × 8 cm × 1 cm

The plastic scintillators are connected to light guides. The light guides are made to guide the scintillation light to the photomultiplier tubes connected.

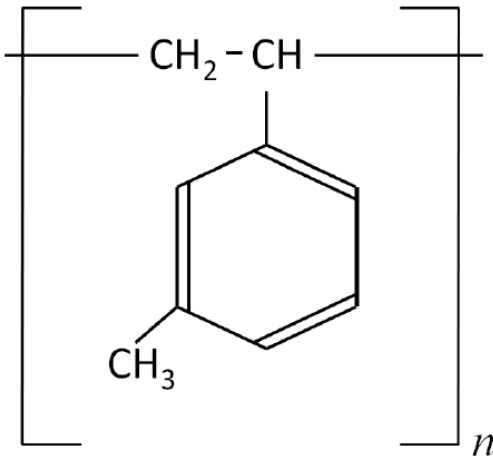


Figure 10: The structural diagram of polyvinyltoluene, the main component of the plastic scintillator.

3.3 Photomultiplier Tube

Photomultiplier tubes create an electronic signal when they detect a photon. Photomultiplier tubes are used to detect weak light signals (~ 100 photons typically from a scintillator) and amplify it ($10^7 \sim 10^9$ electrons) [6].

Photomultiplier tubes consist of 1) a photocathode and 2) an electron multiplier.

1. Photocathode:

The photocathode converts photons to electrons. When a scintillation photon hits the photocathode, an electron is emitted by the photoelectric effect. The electron must overcome an electric potential barrier to escape the photocathode. Because the materials used for the photocathode have a low potential barrier, some electrons with high energy can escape. These electrons are thermionic noise and is a main cause of noise for the present research.

2. Electron Multiplier:

The electron multiplier receives the electrons emitted from the photocathode and amplifies it. The electron emitted from the photocathode is first accelerated by an electric field. The electric field is created by a dynode. The electron is accelerated towards the dynode and hits it. Upon impact, several electrons are released by the dynode and are accelerated again by the next dynode. This process continues for each dynode and the number of electrons increases with each dynode acceleration and hit. The number of electrons created in the electron multiplier depends on the voltage of the electric field. The amplification parameter δ defined as

$$\delta = \frac{\text{electrons emitted by the electron multiplier}}{\text{electrons introduced to the electron multiplier}} \quad (24)$$

is typically proportional to $V^6 \sim V^9$.

Recommended Voltage	-1750 V
Maximum Voltage	-2000 V
Anode Pulse Rise Time	2.1 ns (typical)
Electron Transit Time	29 ns (typical)
Transit Time Spread	1.2 ns (typical)

Table 3: The specifications for the R7724 photomultiplier tube made by Hamamatsu Photonics Inc.

The photomultiplier tubes used in the present research are the R7724 from Hamamatsu Photonics Inc. The specifications of this photomultiplier tube are shown in Table 3.

The schematics of a plastic scintillator connected to a light guide and a photomultiplier tube is shown in Fig. 11.

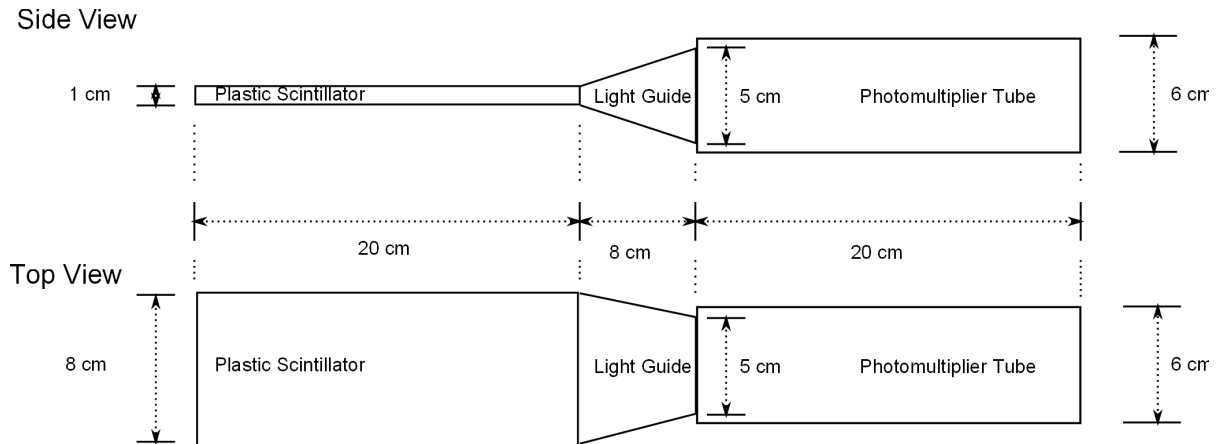


Figure 11: The schematics of a plastic scintillator connected to a light guide and a photomultiplier tube.

3.4 Materials used as stopper

In the present research, the lifetimes of muons in aluminum and iron are measured. Both the aluminum and iron are thin plates. The total thickness can be adjusted by stacking an appropriate number of the thin plates. The dimensions of the thin plates are as follows:

Material	Dimension (Length × Width × Depth)	Density (g/cm ³)	Depth (g/cm ²)
Aluminum	20 cm × 8 cm × 1 cm	2.7	2.7
Iron	20 cm × 8 cm × 0.3 cm	7.9	2.4
Iron	20 cm × 8 cm × 0.2 cm	7.9	1.6

3.4.1 Interaction of muons with matter

When muons come into condensed matter, muons deposit energy into the matter and may eventually stop inside the matter. The muons deposit energy through electromagnetic interactions.

There is not much difference between the interaction of positive and negative muons with matter when the muons have a kinetic energy more than a few keV [3]. The main source of energy loss at these energies is ionization. The muons excite an electron in the atom of the matter and cause the atom to ionize. The energy loss in ionization is described in the Bethe-Bloch equation [1]

$$-\frac{dE}{dx} = D\rho \frac{Z}{A} z^2 \frac{1}{\beta^2} \left[\ln \left(\frac{2m_e \gamma^2 v^2}{I} \right) - \beta^2 + \frac{\delta}{2} \right] \quad (25)$$

where

$$D = \frac{e^4 n}{4\pi \epsilon_0^2 m_e c^2 \rho} \frac{A}{Z} \simeq 0.3071 \text{ MeVcm}^2/\text{g}. \quad (26)$$

$n = \rho \left(\frac{Z}{A} \right) N_A$, N_A is the Avogadro number, $m_e = 0.511 \text{ MeV}/c^2$, e is the elementary charge, ρ is the density of the matter, Z is the atomic number of the matter, A is the atomic weight of the matter, $\beta = v/c$, I is the mean ionization potential, and $\gamma = 1/\sqrt{1 - \beta^2}$. The δ is a correction of no more than several percent. The mean ionization potential for each material is approximated using the atomic number Z by the equation,

$$I \sim 16Z^{0.9} \text{ [eV]}. \quad (27)$$

The values of atomic number Z , atomic weight A , ρ , I for aluminum and iron are shown below.

Material	Z	A	ρ (g/cm ³)	I (eV)
Aluminum	13	27	2.7	161
Iron	26	56	7.9	300

The energy loss in Eq. 25 is expressed using β . It is more useful if expressed in kinetic energy T . Using the relation

$$T = E - m_\mu c^2 \quad (28)$$

the β^2 is

$$\beta^2 = \frac{\frac{T}{m_\mu c^2} \left(\frac{T}{m_\mu c^2} + 2 \right)}{\left(\frac{T}{m_\mu c^2} + 1 \right)^2} \quad (29)$$

for kinetic energy T and mass of muon m_μ , and therefore Eq. 25 can be re-written as

$$\frac{dE}{dx}(T) = D\rho \frac{Z}{A} z^2 \left(\frac{\left(\frac{T}{m_\mu c^2} + 1 \right)^2}{\frac{T}{m_\mu c^2} \left(\frac{T}{m_\mu c^2} + 2 \right)} \ln \left[\frac{2mc^2}{I} \frac{T}{m_\mu c^2} \left(\frac{T}{m_\mu c^2} + 2 \right) \right] - 1 + \frac{\delta}{2} \right) \quad (30)$$

Eq. 30 is used to calculate the stopping power of materials for muons.

3.4.2 Interaction of electrons with matter

Electrons have a much smaller mass than muons. The energy loss for electrons in matter is not the same as muons for this reason. Electrons are deflected by the atomic nucleus and lose energy by emitting electromagnetic radiation. As a result, the energy loss for electrons in matter cannot be expressed by the Bethe-Bloch equation.

The ESTAR database compiled by the National Institute of Standards and Technology (NIST) [8] provides data on the energy loss of electrons in matter. The stopping power $-\frac{dE}{dx}$ of iron and aluminum for electrons is shown in Fig. 12.

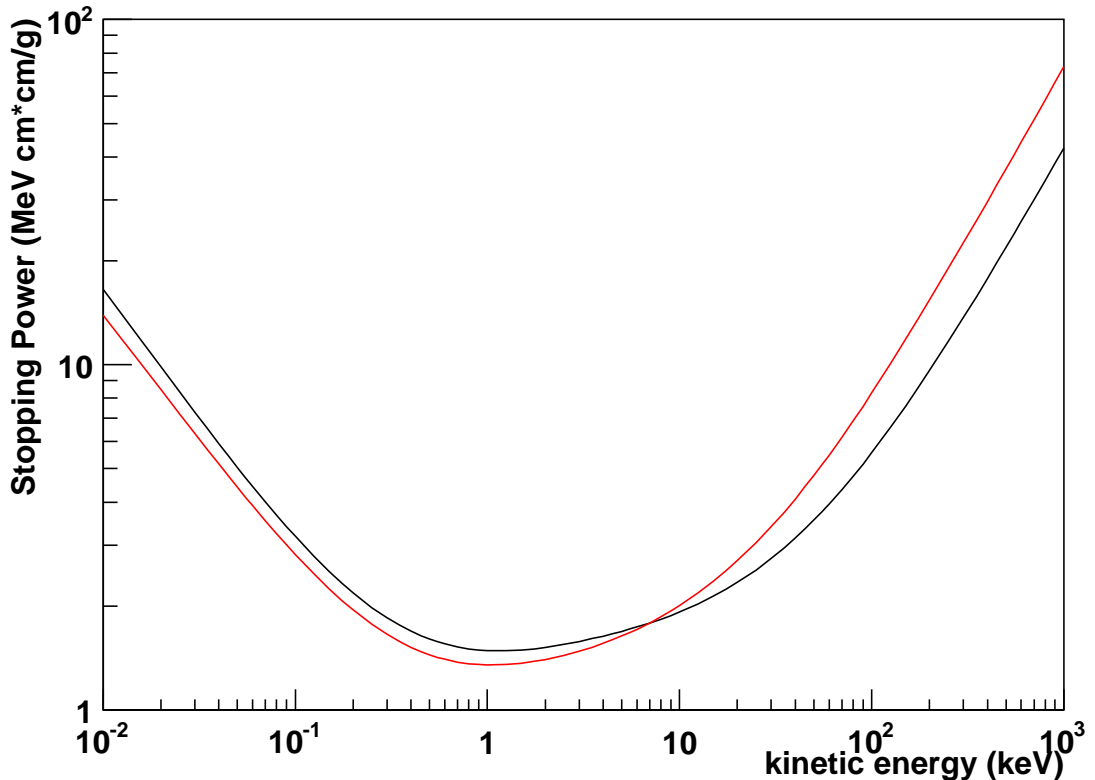


Figure 12: The stopping power of iron and aluminum for electrons. The black curve is the stopping power for aluminum, and the red curve is the stopping power for iron.

3.4.3 Optimization of material thickness

The thickness of the stopper material is determined by matching the area density of the materials. The area density of the materials were made to be close to the area density of a 10 cm thick plastic scintillator block used in earlier experiments [1]. Table 4 shows the thickness and the area density of the materials used in the present experiment.

Material	Density (g/cm ³)	Thickness (cm)	Area Density (g/cm ²)
Plastic (polyvinyltoluene)	1.0	10	10
Aluminum	2.7	3	8.1
Iron	7.9	1.3	10

Table 4: The material, density (g/cm³), thickness (cm) and area density (g/cm²) for the stopper material used in the present experiment.

3.5 Electronics and Circuitry

3.5.1 Modules

The signals are handled by NIM modules and data are stored in a computer. The NIM modules used are listed below.

1. Discriminator

Discriminators turn analog signals to digital signals by accepting an analog signal larger than the preset threshold and emitting a digital signal of variable width. The discriminator used in the present experiment is N-TM 405 8CH from Technoland Co. The discriminator is used to turn the analog signal created by the photomultiplier tubes into digital signals and also to reduce low-level background noise. The setting for the discriminator threshold is explained in chapter 4.

2. Coincidence Module

Coincidence modules emit a variable width digital signal when two or more signals are input simultaneously. Coincidence modules also have a veto input. When a veto signal is input simultaneously with other signals, the coincidence does not emit a digital signal. The module used in the present experiment is N-TM 103 3CH 4-Fold Coincidence by Technoland Co. The coincidence module generates a logic AND signal. The coincidence module is used to create the start signal and the stop signal for the TAC and reduce backgrounds.

3. FAN IN/OUT

FAN IN/OUT modules emit a digital signal when a signal is input into either one of its inputs. The FAN IN/OUT module used in the present experiment is MODEL 740 QUAD LINEAR FAN-IN/FAN-OUT from PHILLIPS SCIENTIFICS Inc. The FAN IN/OUT generates a logic OR signal. This is used to make the stop signal combining the signals from the top two and bottom two plastic scintillators.

4. Time to Analog Converter (TAC)

Time to Analog Converters emit an analog pulse height with a pulse height corresponding to the length of the time difference between the start and stop signals. When the time difference between the start and stop signals is short, a small pulse

is emitted. When the time difference between the start and stop signals is long, a larger pulse is emitted. The TAC used in the present experiment is Model 566 Time to Amplitude Converter from ORTEC Co. The acceptance time range for the TAC is set before it is used. If a stop signal does not arrive within the time range, then the TAC does not emit a signal. The TAC used in this experiment had two selectors to change the time range: a range switch and a multiplier switch. The time range is set by range (ns) \times multiplier. The available values for the ranges are 50, 100 and 200 (ns), and the available values for the multiplier are 1, 10, 100, 1K, and 10K. In the present experiment, the range is set to 200 ns and the multiplier is set to 100. Therefore, the time range for the TAC is 20 μ s. It is used to record the time difference between the incoming cosmic ray muons and the decay electrons or positrons.

5. Analog to Digital Converter (ADC)

Analog to Digital Converters create a digital signal when an analog signal is input. In the present experiment ADC500 from Laboratory Equipment Co. is used. The ADC takes an analog signal and designates a digital value to the pulse height of the analog signal. The ADC used approximates the analog value to a digital signal in one of 1024 channels. It is used to convert the analog signal from the TAC to a digital signal.

6. Multichannel Analyzer (MCA)

Multichannel analyzers accumulate digital signals for each channel. In the present experiment, MCA510 from Laboratory Equipment Co. is used. It is used to accumulate the digital signals from the ADC to the 1024 channels in order to create the time spectrum.

3.5.2 Circuit

The NIM modules are used to record the time difference between the incoming muon signal and decay electron or positron signal. The circuit is shown in Fig. 14.

The start and stop signals for the TAC are

START	$\#1 \cap \#2 \cap \bar{\#3}$
STOP	$(\#1 \cap \#2 \cap \bar{\#3} \cap \bar{\#4}) \cup (\#3 \cap \#4 \cap \bar{\#1} \cap \bar{\#2})$

The measurement process is as follows:

1. A cosmic ray muon penetrates #1 and #2 scintillators. The signals are emitted from the photomultiplier tubes.
2. If a coincidence is taken, this is the start time for the TAC.
3. The cosmic ray muon slows down in the material and stops. If the muon is a positive muon, it decays and emits a positron. If the muon is negative muon, it forms a muonic atom and either decays and emits an electron or is captured by the nucleus.

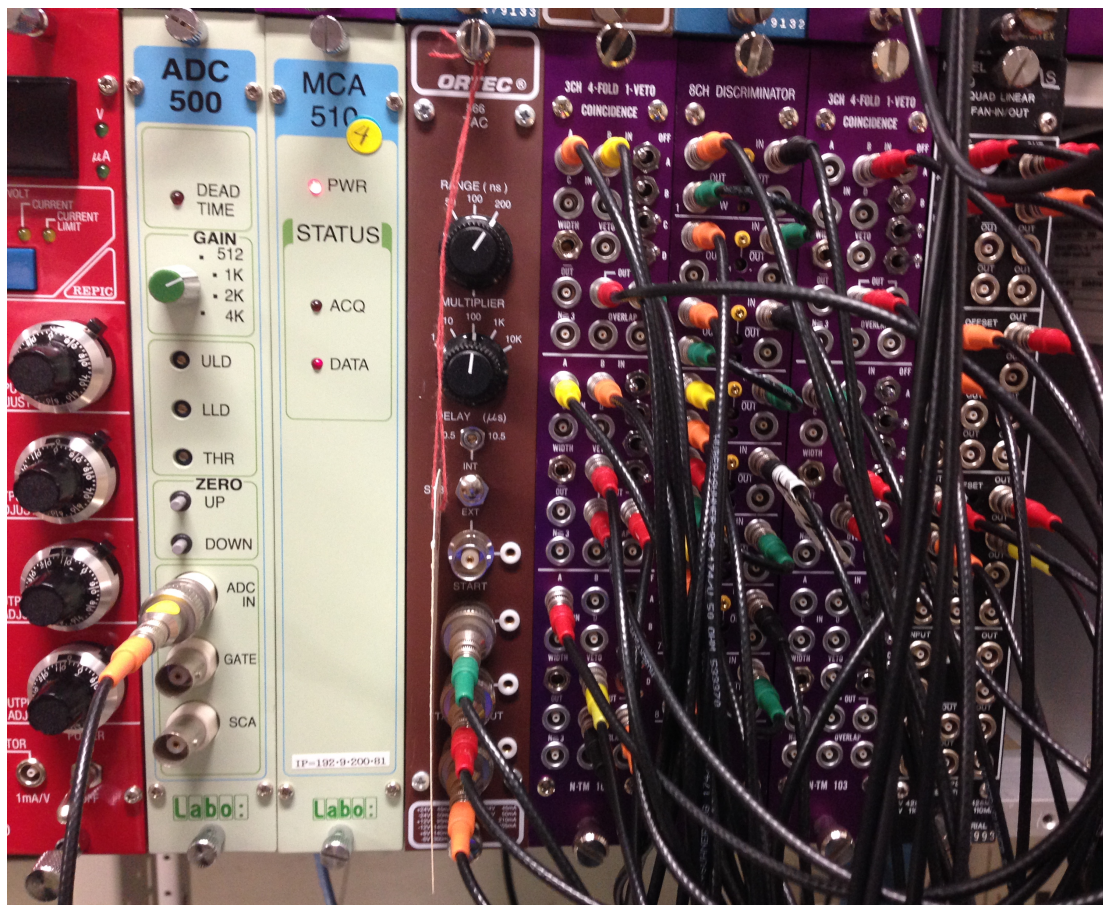


Figure 13: The actual modules used to collect data. From left to right: Analog-to-Digital Converter (ADC), Multichannel Analyzer (MCA), Time-to-Analog Converter (TAC), Coincidence, Discriminator, FAN IN/OUT.

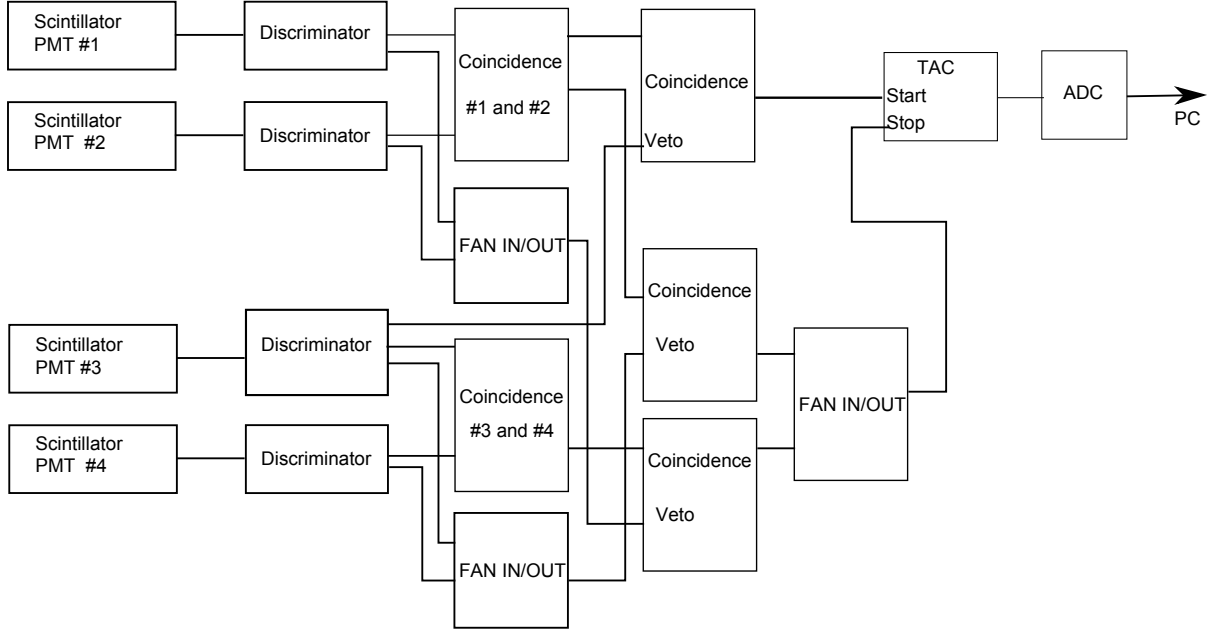


Figure 14: The setup used four photomultiplier tubes. The photomultiplier tubes send an analog signal to the discriminator. The discriminator takes the analog signal and creates a digital signal. The coincidence between #1 and #2 is required. Likewise, the coincidence between #3 and #4 is required.

4. The positron or electron from muon decay penetrates either #1 and #2 or #3 and #4. The signals are emitted from the photomultiplier tubes.
5. If a coincidence is taken, this is the stop time for the TAC.
6. The TAC sends an analog pulse according to the time difference of the start and stop signals.
7. The ADC records the pulse height and sends a digital signal to the MCA.
8. The MCA collects the data and sends it to the PC.

It is important to delay the start signal by several ns to ensure the start signal and the stop signal do not arrive at the TAC simultaneously.

4 Preparations for Measurements

4.1 Time Calibration

Time calibration needs to be done first as the time spectrum is measured by a system of the TAC + ADC + MCA. The relationship between the channel in the MCA, ch , and the time, t (μs), is well expressed with a linear equation

$$t = a \times ch + b \quad (31)$$

where a and b are parameters. These two parameters need to be determined.

The time calibration is done by feeding the start and stop signals of time difference of about 0.2, 1, 2 and 10 μs signals to the TAC + ADC and recording the corresponding channel in MCA.

A clock generator is used to create the pulses. A clock generator creates pulses at a fixed repetition rate. The clock generator can create pulses at a frequency of 10, 100, 500 Hz, 1, 5, 10, 50, 100, 500 kHz, 1, 5, and 10 MHz. In this research, the rates of 5, 1 MHz, 500, and 100 kHz are used. These correspond to 0.2, 1, 2 and 10 μs time periods, respectively.

The clock generator has two output channels. Each channel outputs the same pulse at the same time. One output is used as the stop signal for the TAC. Another output is delayed by 2 ns and used as the start signal for the TAC. The start signal is delayed by 2 ns to ensure the start and stop signals are not input simultaneously. The start signal always arrives at the TAC 2 ns after the stop signal with this configuration. The circuit for the time calibration is shown in Fig. 15.

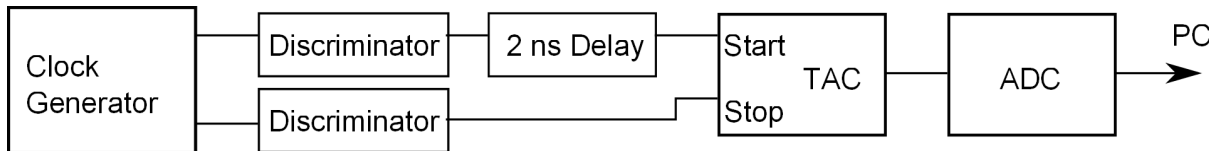


Figure 15: The circuit used for the time calibration. The clock generator created signals for 0.2, 1, 2, and 10 μs . Two signals are used. One is used as the stop signal, while the other is delayed by 2 ns and is used as the start signal. The start signal is delayed by 2 ns to ensure the TAC does not record 0 ns for the time difference between the start and stop signals.

The corresponding channel in ADC for each time pulse is recorded. The time differences between the start and stop signals are 98 ns, 198 ns, 0.998 μs and 9.998 μs because of the 2 ns delay for the start signal. The time chart for the start and stop signals is shown in Fig. 16 for the case of 1 μs generator pulse.

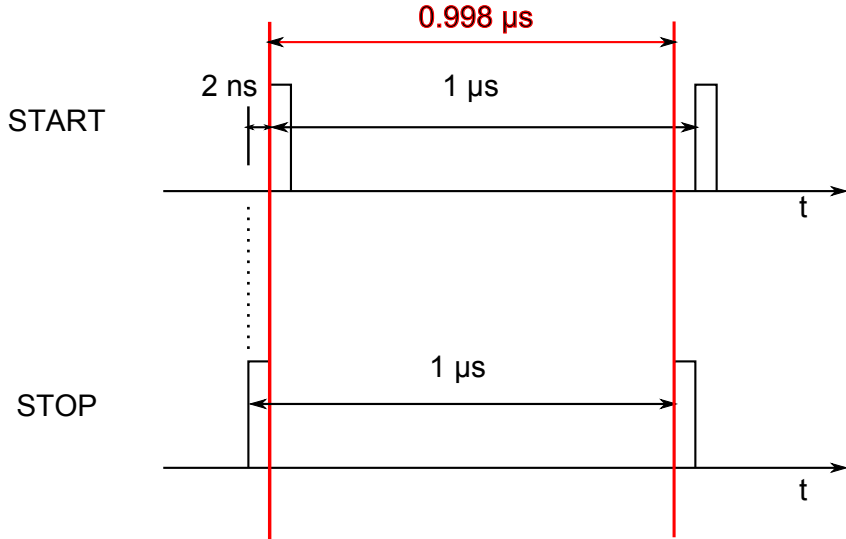


Figure 16: The time chart for the start and stop signals for the time calibration. The start signal is delayed by 2 ns to prevent the start and stop signals from arriving at the TAC simultaneously. As a result, the time difference recorded in the TAC is 0.998 μ s.

The results are shown in Table 5

Time (μ s)	Channel
0.198	18
0.998	59
1.998	111
9.998	526

Table 5: The time difference of the pulses and the corresponding channel recorded on the TAC + ADC.

The parameters a and b of the time calibration are determined by plotting the points on a time-to-channel graph, and fitting with Eq. 31. The graph and the result of the fit is shown in Fig. 17.

The result of the time calibration is shown in Table 6.

By using these values, the time calibration is

$$t = 0.019282 \times ch - 0.144 \text{ } \mu\text{s.} \quad (32)$$

In the present research, this equation is used to convert the MCA channels to time.

4.2 Discriminator Threshold

The analog signals from the photomultiplier tubes are sent to the discriminators. The discriminators allow a pulse greater than the threshold level to pass as a digital signal.

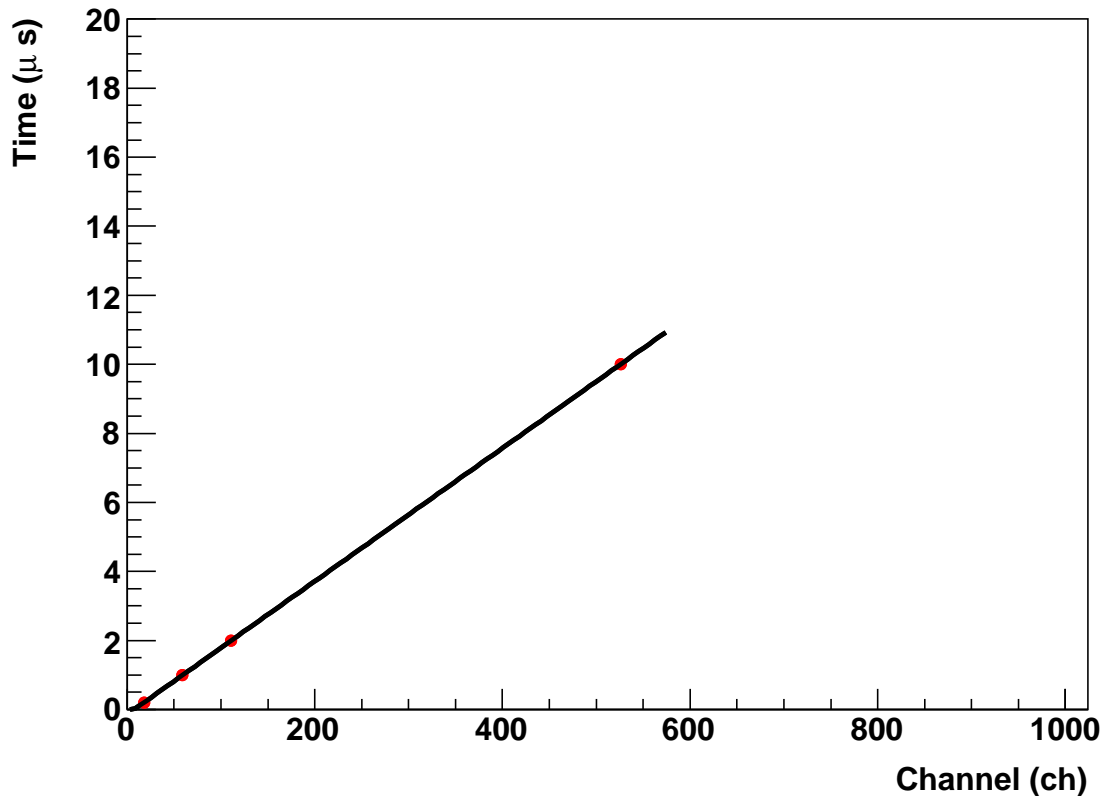


Figure 17: The time calibration graph for the setup. Signals for $0.2 \mu\text{s}$, $1 \mu\text{s}$, $2 \mu\text{s}$, and $10 \mu\text{s}$ were measured. The points are fitted with a line. The time calibration obtained $t = 0.019282 \times ch - 0.144$

parameter	value
a	0.0192824 ± 0.000012
b	-0.1440 ± 0.0032

Table 6: The values for the parameter a and b of the time calibration.

The threshold for the discriminators must be set at an appropriate level. The discriminator should be able to remove noise while also not removing true muon or electron signals. This appropriate level is determined by using a ^{90}Sr beta ray source as a reference. The maximum energy E_{max} of the beta ray from a ^{90}Sr beta ray source is

$$E_{max} = 2.23 \text{ MeV} \quad (33)$$

In this research, the threshold is set to be 1/3 of the maximum pulse height from the detection of the beta ray from a ^{90}Sr beta ray source. This is appropriate because a muon passing through the plastic scintillators of 1 cm thickness also deposits 2 MeV. The pulses of the beta ray are observed by an oscilloscope. The screen of the oscilloscope is shown in Fig. 18.

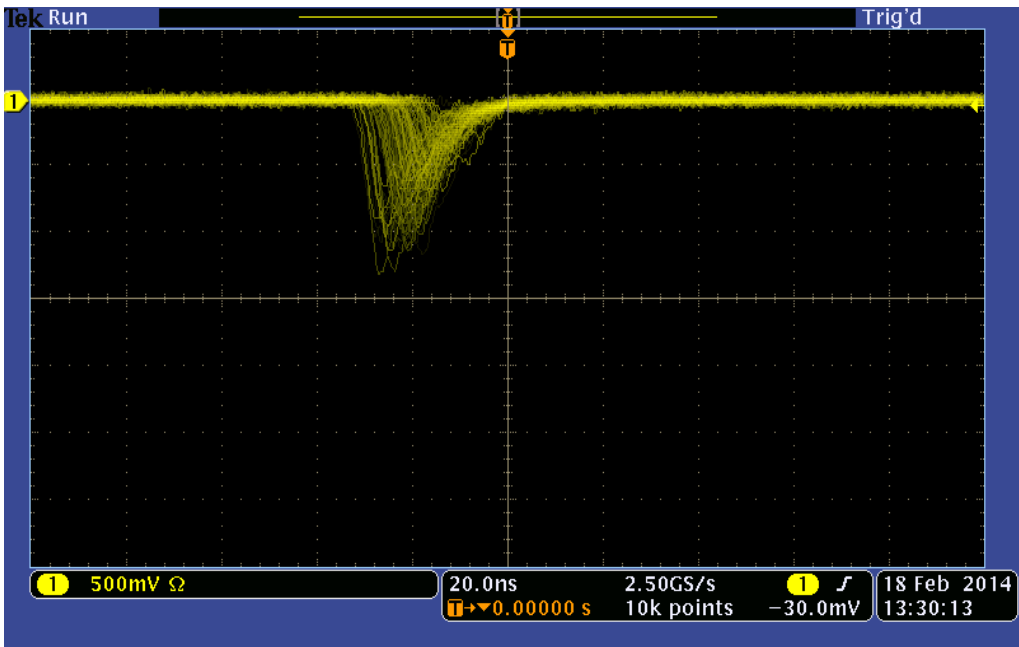


Figure 18: The pulses of beta rays from the ^{90}Sr beta ray source. The threshold for the discriminators used in the setup is set to be about 1/3 of the highest pulse from the ^{90}Sr beta ray source. The yellow curves are pulses from the detection of beta rays from the ^{90}Sr beta ray source.

The maximum voltage V_{max} of the pulses from the detection of the beta rays is

$$V_{max} = 1.5 \text{ V.} \quad (34)$$

Therefore, in this research, the threshold for the discriminators is set at 500 mV.

4.3 Coincidence, Anti-coincidence and Accidental Coincidence

Coincidence is used for the stop signal as well as the start signal to reduce background noise.

4.3.1 Coincidence and Anti-coincidence

The pulse width of each photomultiplier signal for the coincidence and anti-coincidence from the discriminator is optimized to reduce background. The overlap width necessary for the coincidence module to recognize a coincidence is 3 ns. The discriminator pulses for each photomultiplier tube need to be at least 3 ns wide. To ensure the the pulses are counted as coincidence with the appropriate overlap, the pulses are set to have a width of 10 ns. The pulses used for the anti-coincidence are set at 70 ns.

4.3.2 Accidental Coincidence

Accidental coincidence is a coincidence signal created by a simultaneous input of noise into the coincidence module from two photomultiplier tubes. The rate of accidental coincidence R_{acc} (Hz) is expressed as

$$R_{acc} = R_1 \cdot R_2 \cdot (h_1 + h_2 - 2h_3) \quad (35)$$

where R_1 (Hz) is the rate of photomultiplier tube 1, R_2 (Hz) is the rate of photomultiplier tube 2, h_1 (s) and h_2 (s) are the pulse width of the signals from the discriminators of photomultiplier tubes 1 and 2, respectively, and h_3 is the minimum pulse width of the coincidence. The rate of accidental coincidence not only depends on R_1 and R_2 , but depends on the discriminator pulse width of each photomultiplier tube. If the discriminator pulse width is widened to ensure coincidence is appropriately taken, then the accidental coincidence will increase.

5 Muon Lifetime Measurements

The lifetime of muons are measured by recording a time spectrum of muon decay.

In case of muon lifetime measurements with either only positive muons or only negative muons, the spectrum is fitted with the function:

$$\frac{N_0}{\tau_\mu} \exp(-t/\tau_\mu) + C. \quad (36)$$

N_0 is the total number of detected muon decay, τ_μ is the lifetime of muons, C is a constant for the background, and t is time. Because cosmic ray muons are a mixture of both positive and negative muons, the muons stopped in the materials are a mixture of positive and negative muons. The decay of positive and negative muons are independent and emit electrons or positrons independently. Therefore the decay time spectrum is fitted with the sum of two exponential functions

$$\frac{N_0^+}{\tau^+} \exp(-t/\tau^+) + \frac{N_0^-}{\tau^-} \exp(-t/\tau^-) + C. \quad (37)$$

The N_0^+ is the total number of detected positive muon decay, τ^+ is the lifetime of positive muons, N_0^- is the total number of detected negative muon decay, τ^- is the lifetime of negative muons, and C is a constant for the background. The first term is the decay of positive muons, and the second term is the decay of negative muons.

The lifetime of muons in materials is measured in order to 1) determine the positive muon lifetime and also to 2) test whether the negative muon lifetime can be observed.

5.1 Positive Muon Lifetime Measurement

5.1.1 Measurement

The lifetime of positive muons is determined by measuring the lifetime of muons in iron. The idea is to measure the lifetime after the negative muons have decayed as the lifetime of negative muons is expected to be only 0.20 μ s. The setup used for the measurement is shown in Fig. 19.

The time spectrum of muon decay was accumulated for 622,898 sec. This is equivalent to around 173 hours. The total number of accumulated events is 646. The time spectrum obtained from the measurement is shown in Fig. 20.

5.1.2 Fit

The time spectrum of muon decay in iron is fitted from 1.0 μ s up to 10 μ s.

The time spectrum of muon decay in iron is fitted from 1.0 μ s in order to remove the component of negative muon lifetime. The lifetime of negative muons in iron is expected

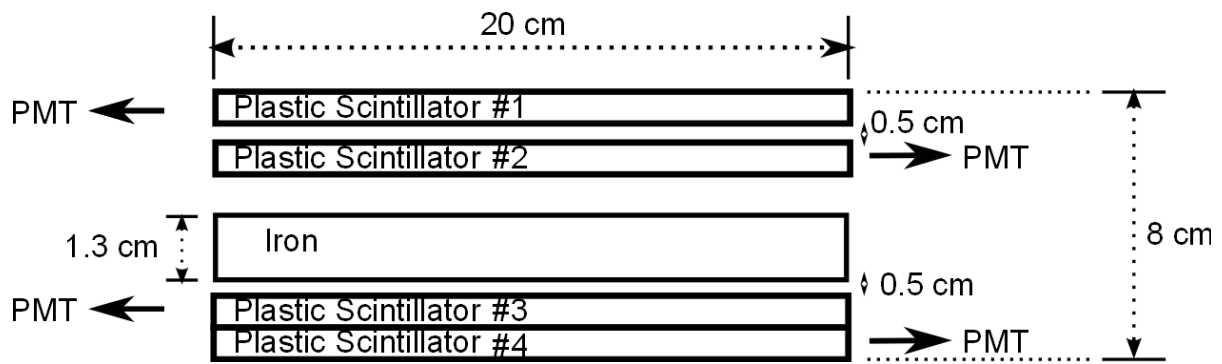


Figure 19: The setup used to observe the positive muon lifetime. The iron used was 1.3 cm thick. The iron was placed on a wooden board.

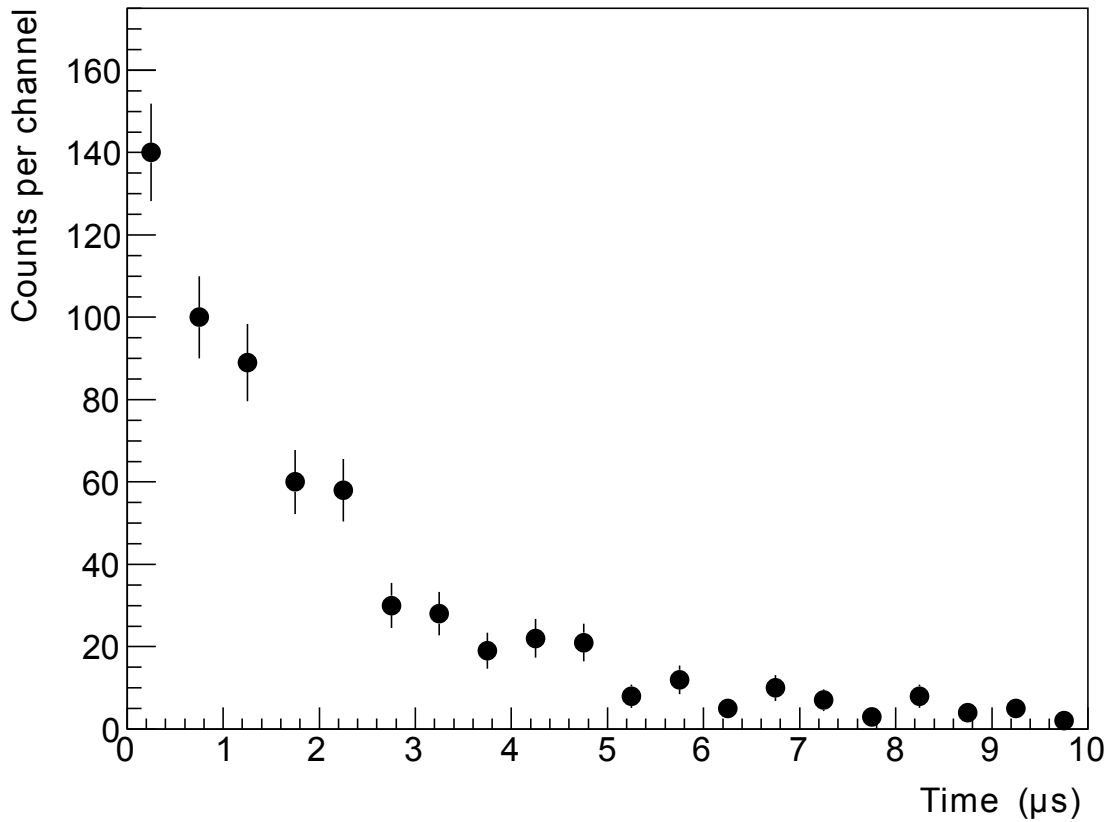


Figure 20: The time spectrum of muon decay in iron. Here, the time spectrum from 0 to $10 \mu\text{s}$ is shown. The total counts from 0 to $20 \mu\text{s}$ are 646.

to be $0.20 \mu\text{s}$. Using Eq. 37, the time spectrum of muon decay in iron is expected to be

$$\frac{N_0^+}{2.2} \exp(-t/2.2) + \frac{N_0^-}{0.20} \exp(-t/0.20) + C. \quad (38)$$

Therefore, the component of negative muon is expected to be much shorter in time compared to the positive muon.

By $1.0 \mu\text{s}$, the component of the negative muon is reduced by a factor of

$$e^{-1.0/0.2} = e^{-5} = 0.0067. \quad (39)$$

The component of negative muons should be negligible compared to the component of positive muons after $1 \mu\text{s}$. By fitting the time spectrum of muon decay after $1 \mu\text{s}$, the second term in Eq. 37 can be ignored.

The time spectrum of muon decay is fitted up to $10 \mu\text{s}$ in order to decrease the error. Specifically, the constant C for background in the Eq. 37 is set at a fixed value. The background is fixed at the average counts per bin from 14 to $20 \mu\text{s}$. Therefore, the time spectrum of muon decay in iron is fitted using the equation:

$$\frac{N_0^+}{\tau^+} \exp(-t/\tau^+) + C(\text{fixed}). \quad (40)$$

where N^+ and τ^+ are the two fitting parameters.

5.2 Negative Muon Lifetime Measurement

5.2.1 Measurement

In the present research, whether the lifetime of negative muons can be observed is tested. The lifetime of muons in aluminum is measured to test this. The lifetime of negative muons in aluminum is expected to be $0.88 \mu\text{s}$ while the lifetime of positive muons is expected to be $2.2 \mu\text{s}$. Therefore, I tested whether the shorter lifetime of the negative muons in aluminum can be observed.

The setup used for the measurement is shown in Fig. 21.

The time spectrum of muon decay was accumulated for 2,672,167 sec. This is equivalent to around 742 hours, or around 31 days. The total number of accumulated events is 3709. It is shown in Fig. 22.

5.2.2 Fit

The time spectrum of muon decay in aluminum is fitted from 0 to $10 \mu\text{s}$. The background is set at a fixed value in the same way as for the positive muon lifetime measurement. The constant C in Eq. 37 is fixed as the average counts per bin from 14 to $20 \mu\text{s}$. The time spectrum therefore is fitted with the following equation,

$$\frac{N_0^+}{\tau^+} \exp(-t/\tau^+) + \frac{N_0^-}{\tau^-} \exp(-t/\tau^-) + C. \quad (41)$$

where N_0^+ , N_0^- and τ_- are the three parameters. The positive muon lifetime is set at 2.3, 2.2, 2.1 and 2.0 and other three parameters are fitted.

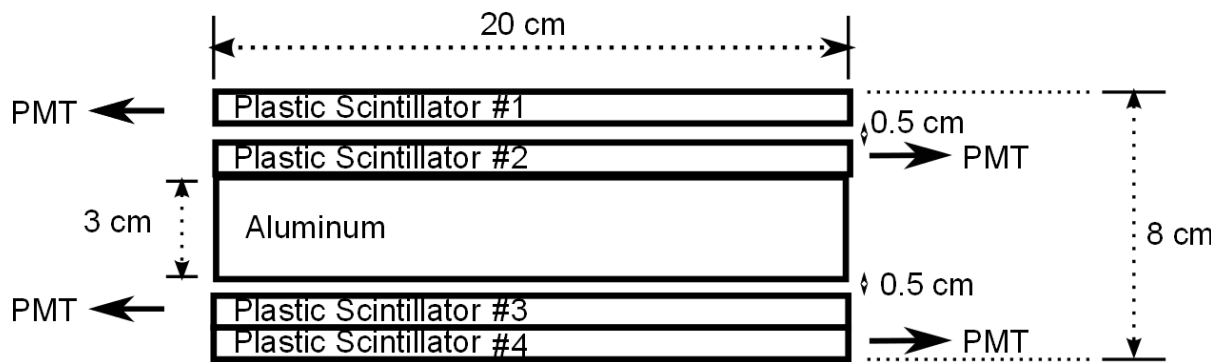


Figure 21: The setup used to test whether the negative muon lifetime can be observed. The aluminum used was 3 cm thick. The aluminum was placed on a wooden board.

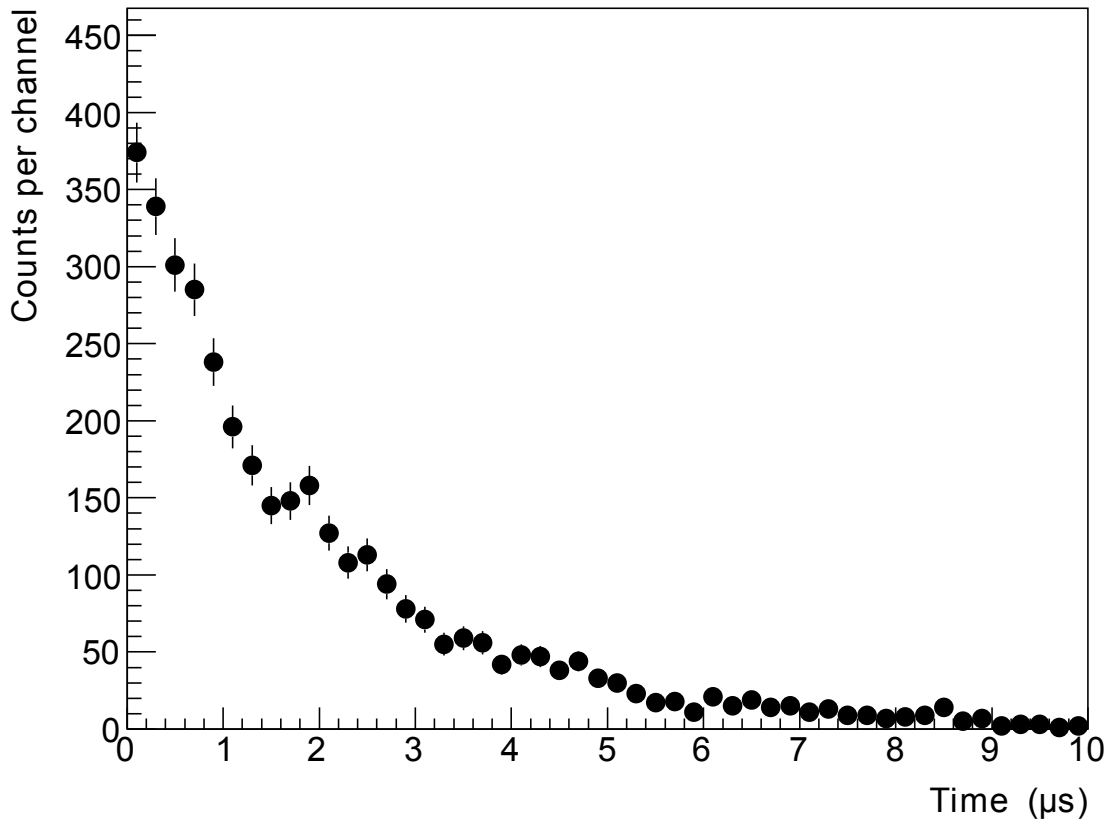


Figure 22: The time spectrum of muon decay in aluminum. Here, the time spectrum from 0 to 10 μ s is shown. The total counts from 0 to 20 μ s are 3709

6 Analysis of Data

6.1 Reduction of Background

One of the main purposes of the present research is to reduce the background in the muon lifetime measurement by use of coincidence both for the start and stop signals. By using my setup, the background is substantially reduced.

The time spectrum of muon decay in aluminum is shown in Fig. 23.

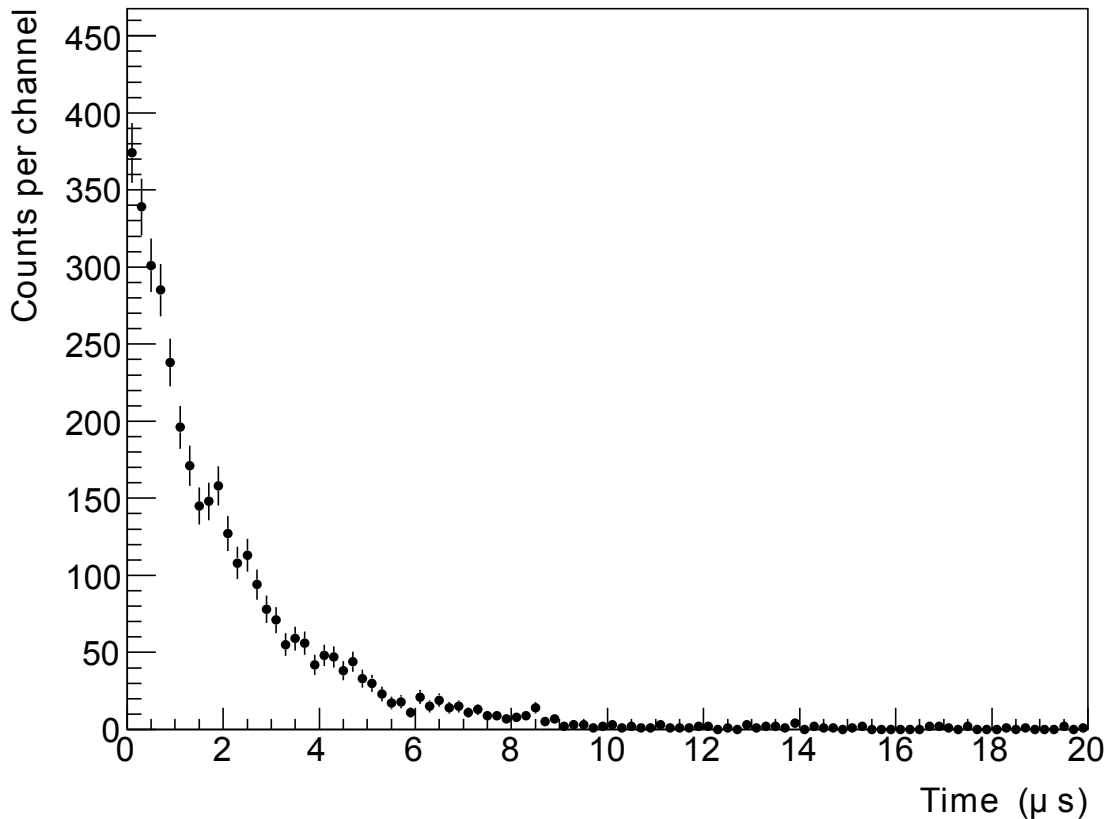


Figure 23: The background was substantially reduced by using coincidence for the stop signal as well as for the start signal. The total counts from 0 to 20 μs is 3709, while the counts from 10 to 20 μs are only 50. The accidental coincidence between the start and stop signals is substantially suppressed.

The time spectrum was accumulated for around 31 days. The total counts are 3709 while the counts from 10 to 20 μs are only 50. The amount of background is evaluated from the counts from 10 to 20 μs . It is reasonable to assume that the same amount of background is present at 0 to 10 μs . Therefore, I define the amount of background as the

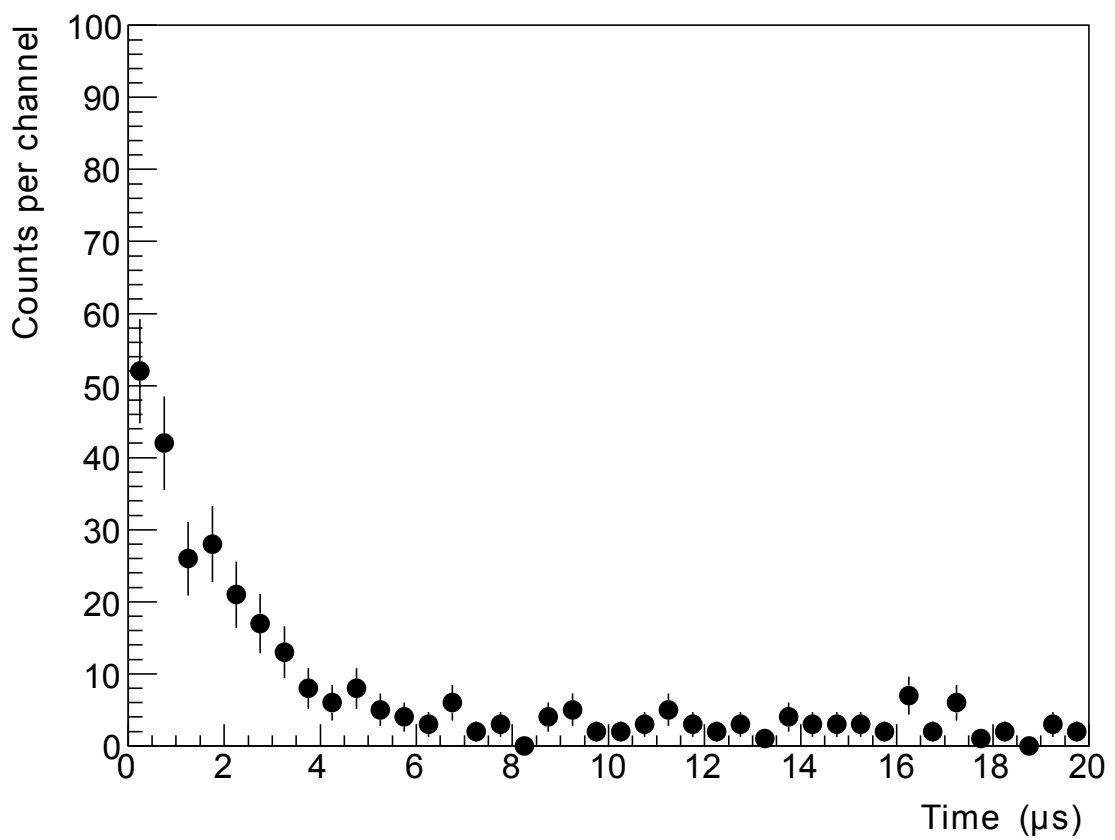


Figure 24: The time spectrum of muon decay in aluminum not using coincidence for neither the start signal nor the stop signal. The counts from 0 to 20 μ s are 313 while the counts from 10 to 20 μ s are 58.

counts from 10 to 20 μs . I define the background ratio $R_{background}$ as

$$R_{background} = \frac{\text{counts from } 10 \text{ to } 20\mu\text{s}}{\text{counts from } 0 \text{ to } 10\mu\text{s} - \text{counts from } 10 \text{ to } 20\mu\text{s}}. \quad (42)$$

The background ratio shows the ratio of the background to the true muon signal. The background ratio of the setup using coincidence is therefore

$$\frac{50}{3609} \simeq 1.4\%. \quad (43)$$

My setup is compared to a setup not using coincidence in order to confirm the effect of coincidence on the background. The setup is exactly the same as the setup using coincidence except for the circuit. The circuit for the setup not using coincidence is shown in Fig. 25.

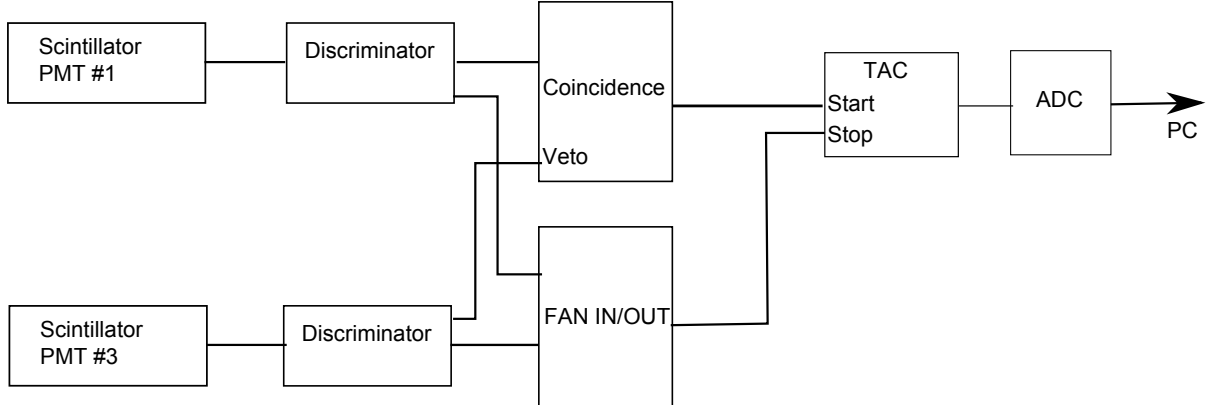


Figure 25: The circuit for the setup not using coincidence. The #1 and #3 from the setup was used. #2 and #4 were not used. The start signal was $\#1 \cap \#3$ while the stop signal was $\#1 \cup \#3$.

The circuit uses the #1 and #3 plastic scintillators and PMTs. The #2 and #4 plastic scintillators and PMTs are removed from the circuit. The start signal was $\#1 \cap \#3$ while the stop signal was $\#1 \cup \#3$.

The time spectrum of muon decay in aluminum with this circuit is shown in Fig. 24. The time spectrum was accumulated for 65000 seconds $\simeq 18$ hours. The total counts are 313 while the counts from 10 to 20 μs are 58. The background ratio is therefore

$$\frac{58}{197} \simeq 30\%. \quad (44)$$

By comparing Eq. 43 and 44, it can be concluded that the background is reduced by a factor of about 21.

6.2 Results of Positive Muon Lifetime Measurement

The positive muon lifetime was measured by fitting the time spectrum of muon decay in iron with the function

$$\frac{N_0^+}{\tau^+} \exp(-t/\tau^+) + C(\text{fixed}). \quad (45)$$

The idea is to measure the lifetime after the negative muons have decayed. Fig. 26 shows the time spectrum of muon decay in iron fitted from 0 to 10 μs , while Fig. 27 shows the time spectrum of muon decay in iron fitted from 1 to 10 μs . The values of the parameters as well as χ^2 and number of degree of freedom (ndf) of the fit are shown in tables.

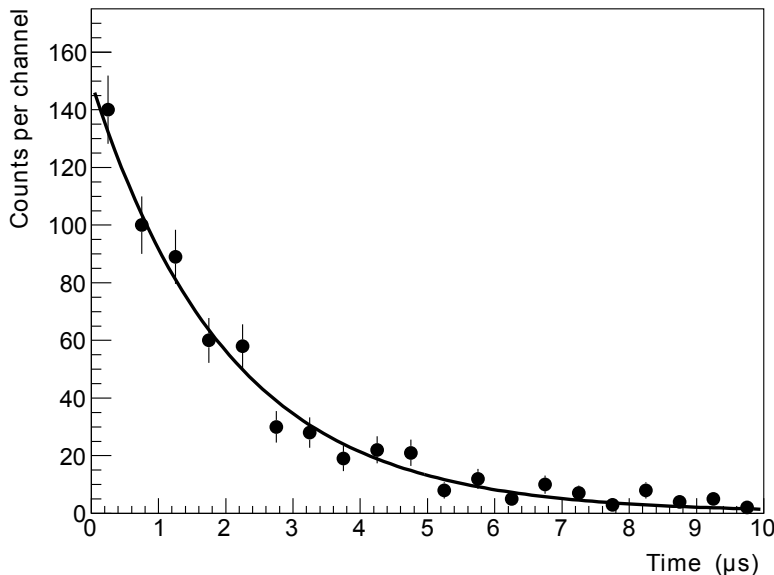


Figure 26: The time spectrum of muon decay in iron fitted from 0 to 10 μs . The fitted lifetime is $2.0 \pm 0.10 \mu\text{s}$.

Table 7: The values of the parameters from the fit to the time spectrum of muon decay in iron from 0 to 10 μs .

Parameter	Value
N_0^+	304.3 ± 12.5
τ^+	$2.039 \pm 0.104 (\mu\text{s})$
C	0.33 (fixed)
χ^2/ndf	21.16/18

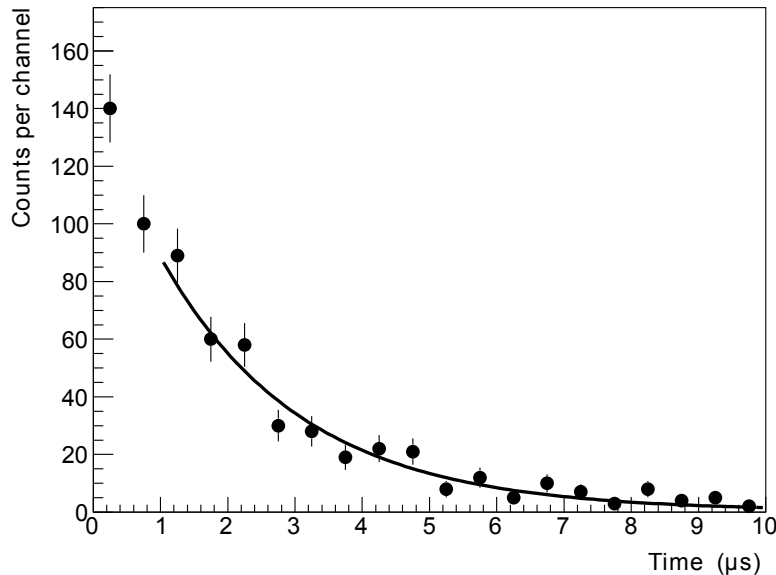


Figure 27: The time spectrum of muon decay in iron fitted from 1 to 10 μs . It was fitted from 1 μs in order to exclude the component of negative muon. The lifetime of negative muons is expected to be 0.20. The fitted lifetime is $2.10 \pm 0.15 \mu\text{s}$.

Table 8: The values of the parameters from the fit to the time spectrum of muon decay in iron from 1 to 10 μs .

Parameter	Value
N_0^+	298.1 ± 18.0
τ^+	$2.097 \pm 0.152 (\mu\text{s})$
C	0.33 (fixed)
χ^2/ndf	20.43/16

The results of the measurement are shown in Fig. 28 and Table 9.

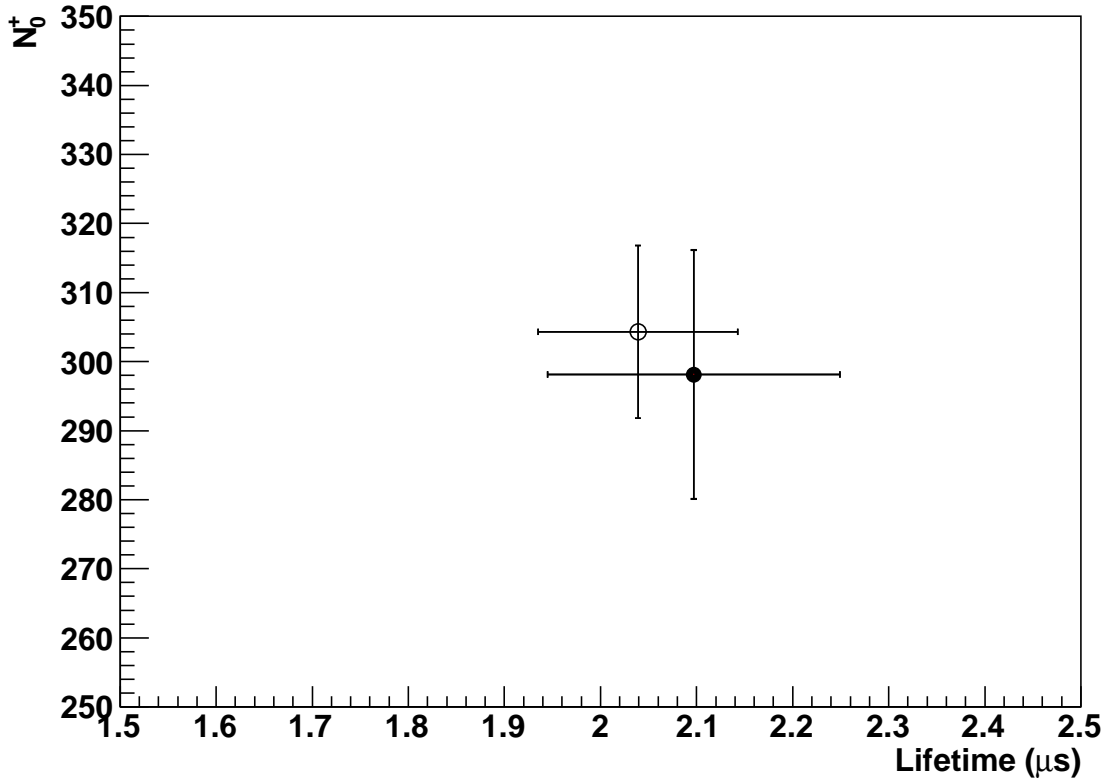


Figure 28: The two sets of the values of N_0^+ and τ^+ obtained from the fits. The open circle is the N_0^+ and τ^+ as a result of the fit from 0 to 10 μs . The black point is the N_0^+ and τ^+ as a result of the fit from 1 to 10 μs .

Table 9: The values of N_0^+ and τ^+ from the two fits.

Fit Range (μs)	Lifetime (μs)	N_0^+
0 - 10	2.04 ± 0.10	304.3 ± 12.5
1 - 20	2.10 ± 0.15	298.1 ± 18.0

The result of the positive muon lifetime is $2.10 \pm 0.15 \mu\text{s}$ in the present experiment. The positive muon lifetime is expected to be $2.2 \mu\text{s}$. The measurement agrees with the expected value.

6.3 Results of Negative Muon Lifetime Measurement

The negative muon lifetime is measured by fitting the time spectrum of muon decay in aluminum with the function

$$\frac{N_0^+}{\tau^+} \exp(-t/\tau^+) + \frac{N_0^-}{\tau^-} \exp(-t/\tau^-) + C(\text{fixed}). \quad (46)$$

where N_0^+ , N_0^- , and τ^- are the three free parameters. The positive muon lifetime was extracted to be $2.10 \pm 0.15 \mu\text{s}$. Therefore, four different values within or close to 1σ of the positive muon lifetime are used for τ^+ : 2.2, 2.1, 2.0 and $2.3 \mu\text{s}$.

6.3.1 Using $2.2 \mu\text{s}$ as the positive muon lifetime

The fitted time spectrum using $2.2 \mu\text{s}$ as the positive muon lifetime is shown in Fig. 29 and the values of the parameters are shown in Table 10.

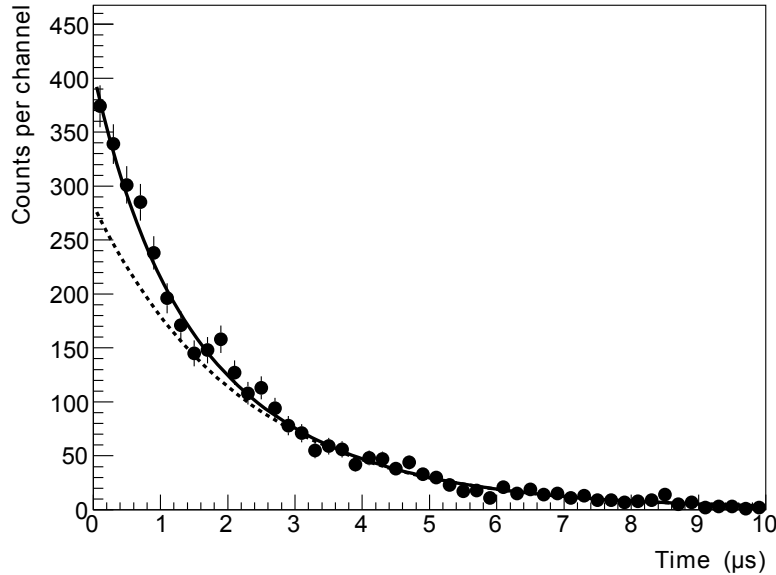


Figure 29: The time spectrum of muon decay in aluminum fitted with the sum of two exponentials. The dotted curve is the component of lifetime fixed at $2.2 \mu\text{s}$ while the solid curve is the sum of the two components. A component with $0.81 \pm 0.11 \mu\text{s}$ is observed.

Table 10: The values of the parameters from the fit to the time spectrum of muon decay in aluminum using $\tau^+ = 2.2 \mu\text{s}$.

Parameter	Value
N_0^+	619.3 ± 12.1
N_0^-	100 ± 6.3
τ^-	$0.809 \pm 0.105 (\mu\text{s})$
C	0.63 (fixed)
χ^2/ndf	57.34/47

The dotted curve is the component of lifetime fixed at $2.2 \mu\text{s}$ while the solid curve is the sum of the two components. The discrepancy at 0 to $2 \mu\text{s}$ suggests the effect of nuclear capture of negative muons. The τ^- was extracted to be $0.81 \pm 0.11 \mu\text{s}$. The negative muon lifetime in aluminum is expected to be $0.88 \mu\text{s}$. The extracted value agrees well with the earlier value.

Using $2.2 \mu\text{s}$ as the positive muon lifetime, hints of the shorter negative muon lifetime are observed. Fig. 30 shows the relation between parameters N_0^+ and τ^+ , and N_0^- and τ^- when using $2.2 \mu\text{s}$ as the positive muon lifetime. The red point in Fig. 30 has a nonzero N_0^- value. The nonzero N_0^- suggests the existence of a component of shorter lifetime.

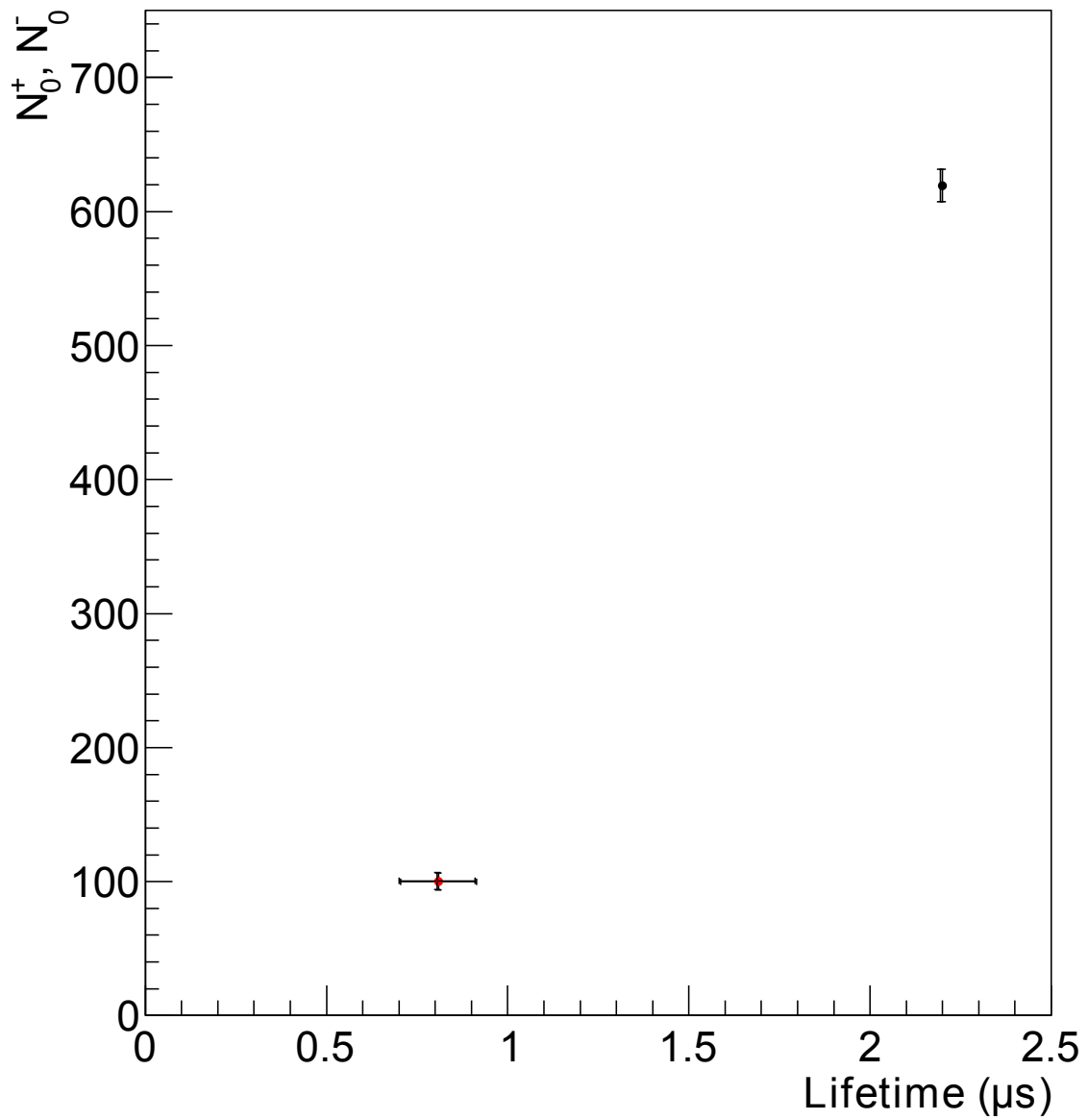


Figure 30: The relation between parameters N_0^+ and τ^+ , and N_0^- and τ^- when using 2.2 μs as the positive muon lifetime. The red point is the N_0^- and τ^- and the black point is the N_0^+ and τ^+ . The nonzero N_0^- suggests the existence of the negative muon lifetime in the time spectrum.

6.3.2 Using $2.1 \mu\text{s}$ as the positive muon lifetime

In the present research, the positive muon lifetime has been extracted to be $2.1 \mu\text{s}$. Here, I tested the fit using $2.1 \mu\text{s}$ as the positive muon lifetime. The fitted time spectrum is shown in Fig. 31 and the values of the parameters are shown in Table 11.

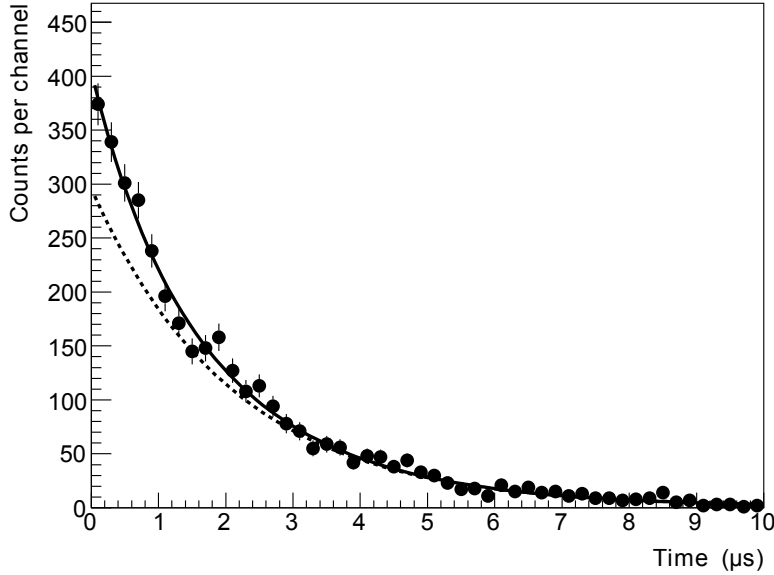


Figure 31: The time spectrum of muon decay in aluminum fitted with the sum of two exponentials. The positive muon lifetime used in this fit is $2.1 \mu\text{s}$. The dotted curve is the component of lifetime fixed at $2.10 \mu\text{s}$ while the solid curve is the sum of the two components. A component with $0.93 \pm 0.13 \mu\text{s}$ is observed.

Table 11: The values of the parameters from the fit to the time spectrum of muon decay in aluminum using $\tau^+ = 2.1 \mu\text{s}$.

Parameter	Value
N_0^+	620.4 ± 12.1
N_0^-	100 ± 74.0
τ^-	$0.9251 \pm 0.1345 (\mu\text{s})$
C	0.63 (fixed)
χ^2/ndf	50.49/47

The error for N_0^- is large in this fit. Fig. 32 shows the relation between the parameters N_0^+ and τ^+ , and N_0^- and τ^- in case of $\tau^+ = 2.1 \mu\text{s}$.

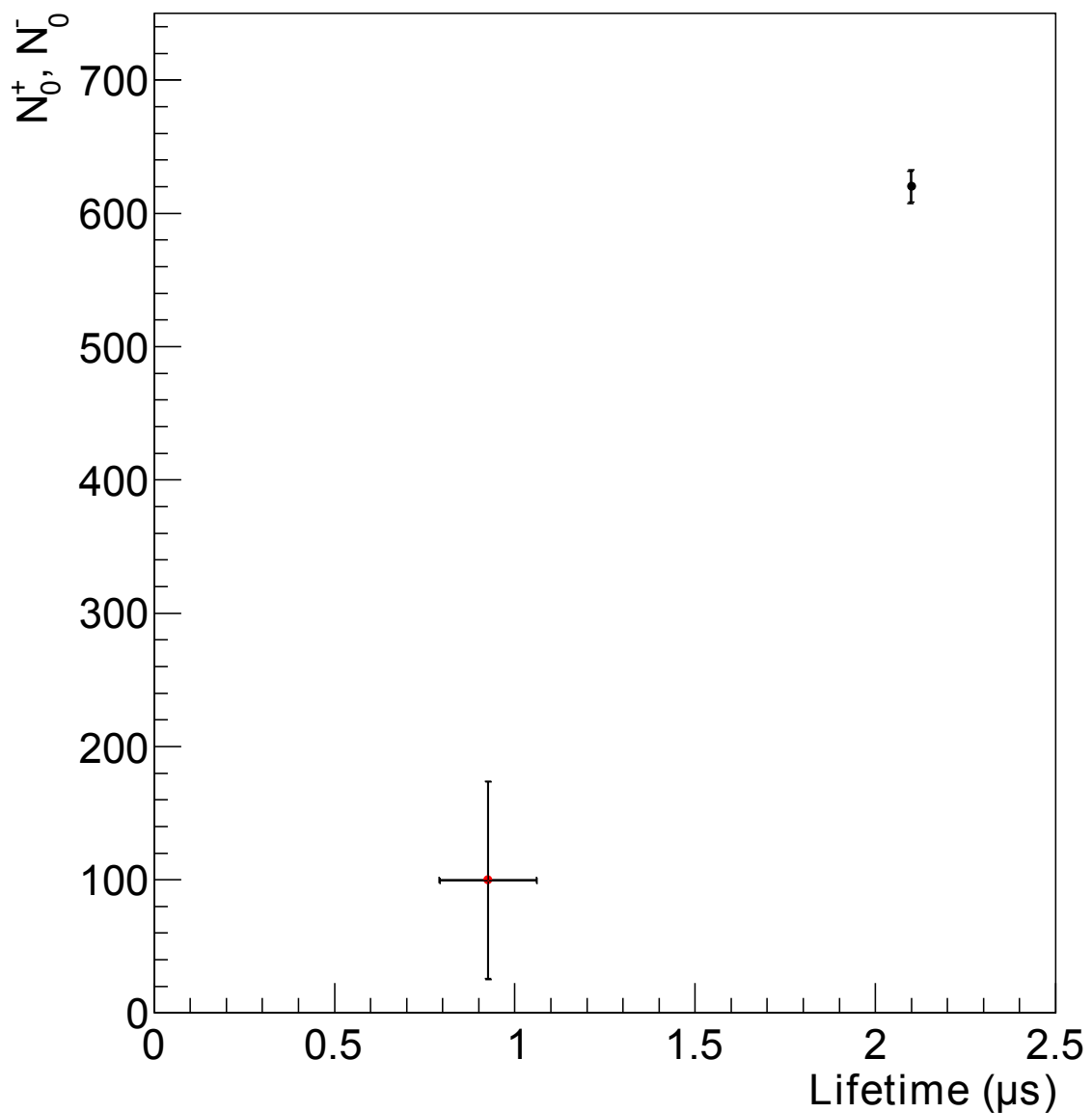


Figure 32: The relation between the parameters N_0^+ and τ^+ , and N_0^- and τ^- when using $2.1 \mu\text{s}$ as the positive muon lifetime. The red point is the N_0^- and τ^- and the black point is the N_0^+ and τ^+ . A large error was observed for N_0^- .

In the case of $\tau^+ = 2.1 \mu\text{s}$, I also fitted N_0^- as a single free parameter with $\tau^- = 0.9251$ and obtained $N_0^- = 100.9 \pm 10.4$. Likewise, I fitted τ^- as a single free parameter with $N_0^- = 100$ and obtained $\tau^- = 0.9251 \pm 0.134$. The large error of N_0^- seems to be the result of correlation between N_0^- and τ^- . The details of the correlation need to be investigated further.

6.3.3 Using $2.0 \mu\text{s}$ as the positive muon lifetime

Here, the negative muon lifetime in case of $\tau^+ = 2.0 \mu\text{s}$ is investigated. The fitted time spectrum is shown in Fig. 33 and the values of the parameters are shown in Table 12. In

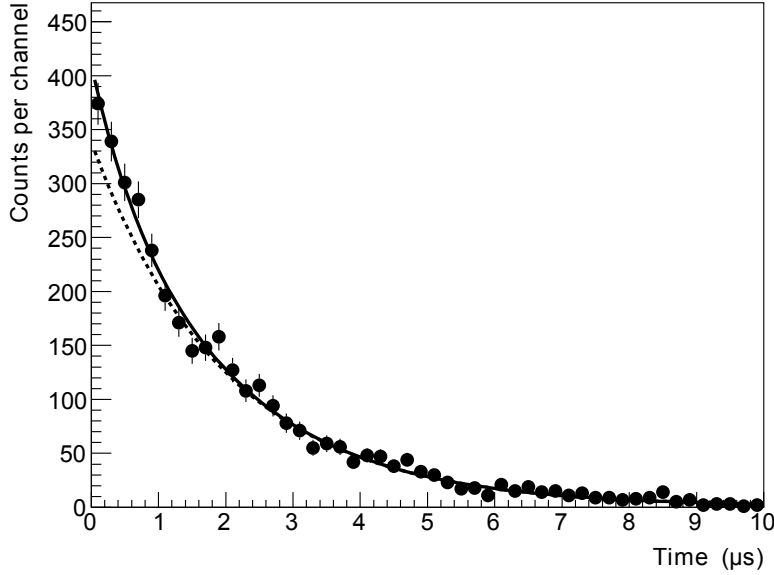


Figure 33: The time spectrum of muon decay in aluminum fitted with the sum of two exponentials. The positive muon lifetime used in this fit is $2.0 \mu\text{s}$. The dotted curve is the component of lifetime fixed at $2.0 \mu\text{s}$ while the solid curve is the sum of the two components. A component with $0.62 \pm 0.28 \mu\text{s}$ is observed.

Table 12: The values of the parameters from the fit to the time spectrum of muon decay in aluminum using $\tau^+ = 2.0 \mu\text{s}$.

Parameter	Value
N_0^+	675.4 ± 24.1
N_0^-	44.54 ± 20.35
τ^-	$0.6199 \pm 0.2753 (\mu\text{s})$
C	0.63 (fixed)
χ^2/ndf	48.94/47

case of $\tau^+ = 2.0 \mu\text{s}$, the error of N_0^- is relatively large.

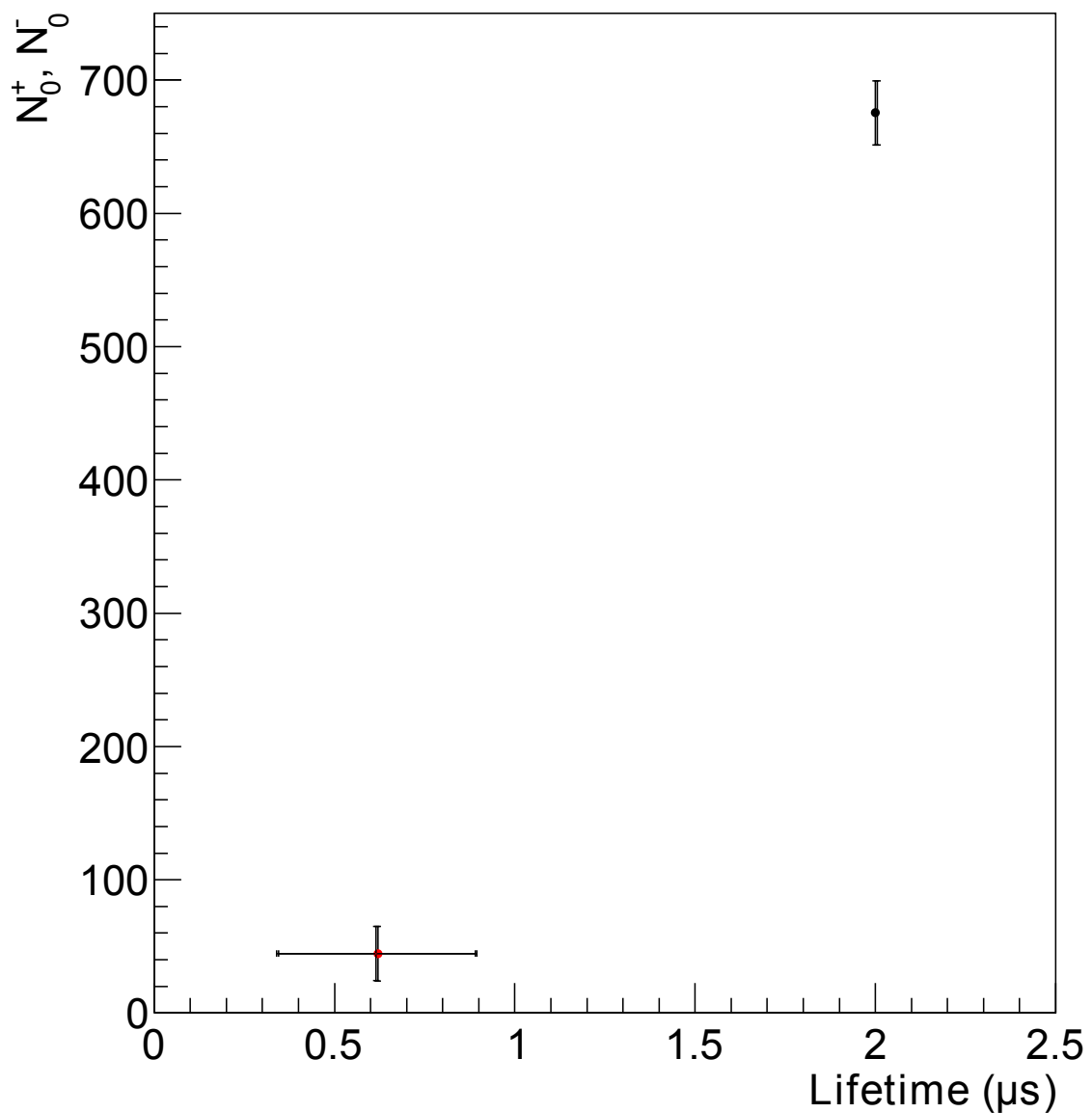


Figure 34: The relation between the parameters N_0^+ and τ^+ , and N_0^- and τ^- when using $2.0 \mu\text{s}$ as the positive muon lifetime. The red point is the N_0^- and τ^- and the black point is the N_0^+ and τ^+ . A large error is observed for N_0^- . N_0^- is 2σ away from zero.

6.3.4 Using $2.3 \mu\text{s}$ as the positive muon lifetime

A fit with $\tau^+ = 2.3 \mu\text{s}$ was also performed. Fig. 35 shows the time spectrum fitted using $\tau^+ = 2.3 \mu\text{s}$. The values of the parameters are shown in Table 13.

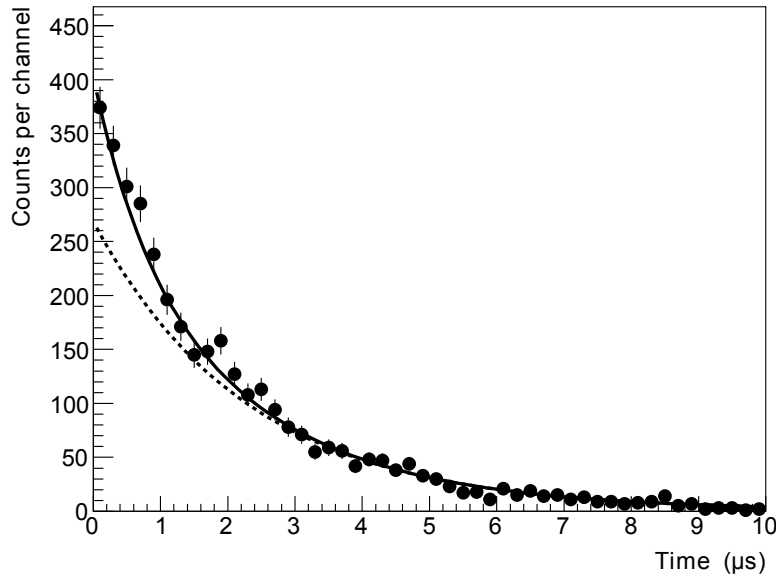


Figure 35: The time spectrum of muon decay in aluminum fitted with the sum of two exponentials. The positive muon lifetime used in this fit is $2.3 \mu\text{s}$. The dotted curve is the component of lifetime fixed at $2.3 \mu\text{s}$ while the solid curve is the sum of the two components. A component with $0.74 \pm 0.09 \mu\text{s}$ is observed.

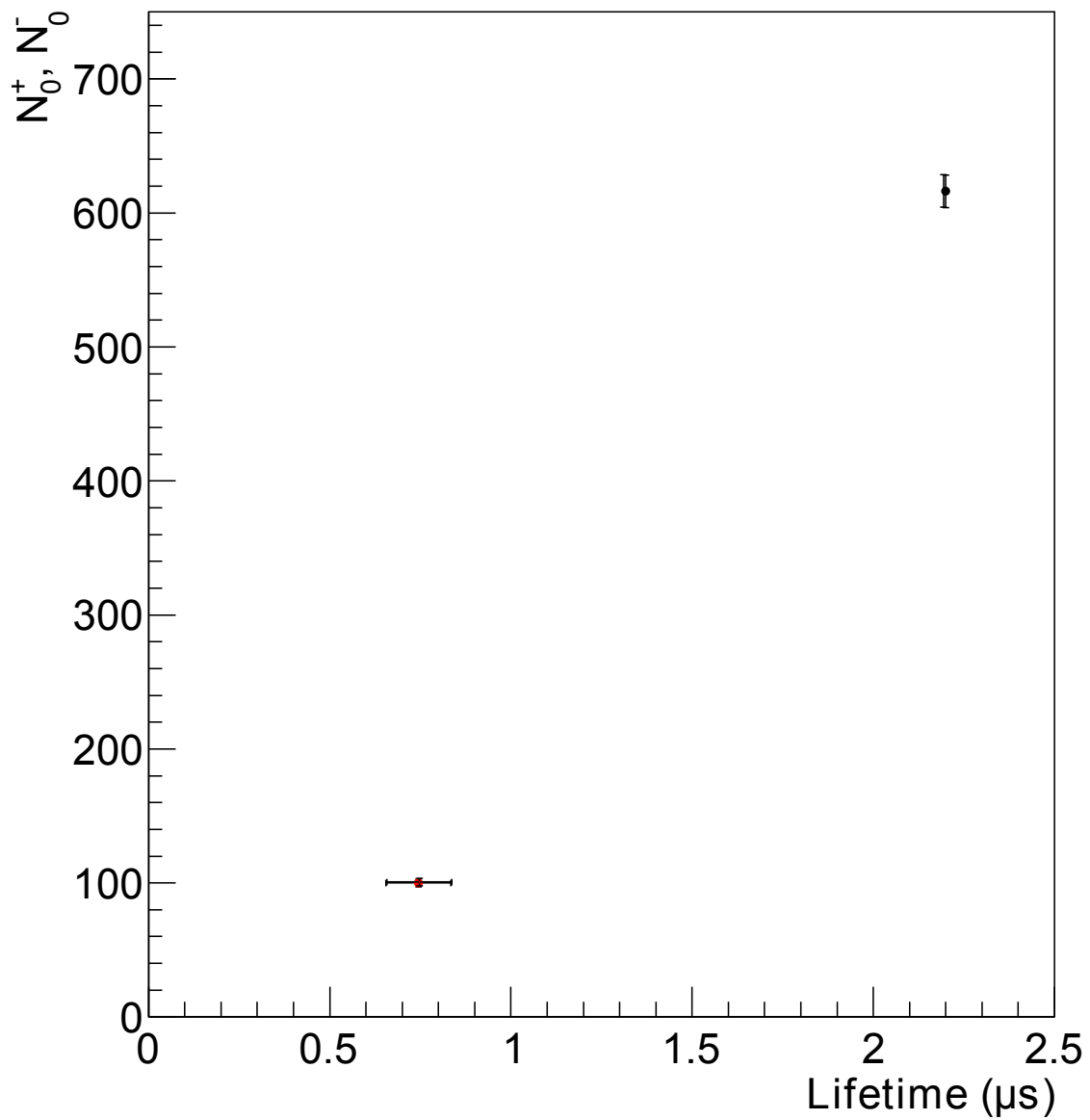


Figure 36: The relation between the parameters N_0^+ and τ^+ , and N_0^- and τ^- when using $2.3 \mu\text{s}$ as the positive muon lifetime. The red point is the N_0^- and τ^- and the black point is the N_0^+ and τ^+ . The χ^2 value is larger than in cases of other τ^+ values.

Table 13: The values of the parameters from the fit to the time spectrum of muon decay in aluminum using $\tau^+ = 2.3 \mu\text{s}$.

Parameter	Value
N_0^+	616.2 ± 12.1
N_0^-	100 ± 2.9
τ^-	$0.7445 \pm 0.0895 (\mu\text{s})$
C	0.63 (fixed)
χ^2/ndf	<u>72.52/47</u>

In Fig. 35, the dotted curve is the component of lifetime fixed at $2.3 \mu\text{s}$ while the solid curve is the sum of the two components. A component with $0.74 \pm 0.09 \mu\text{s}$ is observed. However, in case of $\tau^+ = 2.3 \mu\text{s}$, the χ^2 is larger than in cases of $\tau^+ = 2.2$, 2.10, and 2.0 μs .

7 Conclusion and Summary

In the present research, the lifetimes of muons in aluminum and iron are measured to test whether the decays of positive and negative muons in materials can be observed. Cosmic ray muons are a mixture of both negative and positive muons. Positive muons always have the lifetime of $2.2 \mu\text{s}$ whether they are in matter or not. Negative muons have a shorter lifetime due to the formation of muonic atoms and subsequent nuclear capture. I fabricated a setup to measure the lifetime of muons in aluminum and iron. Using this setup, I performed the following:

- Coincidence for both the start and the stop signals was used to reduce background. Using my setup, the background was substantially reduced.
- The setup was rearranged from earlier experiments so that the materials used as stopper can be easily exchanged. In the present experiment, iron and aluminum can be easily exchanged.
- The lifetime of positive muons was determined by measuring the lifetime of muons in iron.
 - By fitting the time spectrum of muon decay in iron from $1 \mu\text{s}$, the lifetime of positive muons was extracted to be $2.10 \pm 0.15 \mu\text{s}$.
- The lifetime of negative muons was determined by measuring the lifetime of muons in aluminum. The time spectrum was fitted as a sum of two exponential functions.
 - By using $2.2 \mu\text{s}$ as the lifetime of positive muons, a hint of shorter lifetime was observed. The negative muon lifetime was extracted to be $0.81 \pm 0.11 \mu\text{s}$. This agrees well with earlier values. The component of negative muons was shown to be nonzero.
 - By using 2.1 or $2.0 \mu\text{s}$ as the lifetime of positive muons, a large error for the component of negative muons was observed, and further investigation is needed.
 - With $2.3 \mu\text{s}$ as the lifetime of the positive muon the χ^2 value was large. The $2.3 \mu\text{s}$ does not seem to be appropriate to be used in the fit.

To summarize, I learned about the basic of plastic scintillators, coincidence, anti-coincidence and accidental coincidence in the experiment. I measured the positive muon lifetime to be $2.10 \pm 0.15 \mu\text{s}$ using iron as stopper. Hints for negative muon decay with a shorter lifetime were obtained using aluminum as stopper.

Acknowledgements

I would like to express my deepest gratitude to my supervisor, Prof. Toshi-Aki Shibata. He suggested me to do this experiment and gave me guidance throughout my research. I would also like to express my gratitude to Assistant Professor Ken-ichi Nakano for his guidance and advice.

I would like to acknowledge the support of Rui Sanada for his valuable assistance and advice. I would also like to thank all the other members of Shibata-Lab of Tokyo Tech for their insightful advice and help. I could not do this work without the support of all the people mentioned above. I would once again like to express my deep gratitude to all.

References

- [1] 真田星 「ミューオン寿命測定のための同時計測と偶発的同時計測の研究」 東京工業大学理学部物理学科柴田研究室 2013 年度卒業論文
- [2] B. Pohv 他著、柴田利明訳 「素粒子・原子核物理入門」 丸善出版 (2012)
- [3] K. Nagamine, *Introductory Muon Science*. Cambridge University Press (2003).
- [4] T. Suzuki and D.F. Measday, *Total nuclear capture rates for negative muons*. Physical Review C Volume 35, Number 6 (1987)
- [5] J. Beringer *et al.*, 27. *Cosmic Rays* Physical Review D86, 010001 (2012) and update for the 2014 edition. (2013).
- [6] G. F. Knoll, 木村逸郎/阪井英次訳, 「放射線計測ハンドブック」 日刊工業新聞社 (2001).
- [7] NIST (National Institute of Standards and Technology) the ESTAR program, <http://physics.nist.gov/PhysRefData/Star/Text/ESTAR.html>
- [8] 岡村勇介 「荷電粒子の物質中のエネルギー損失と飛程」 東京工業大学理学部物理学科柴田研究室 2009 年卒業論文